The Drosophila Baramicin polypeptide gene protects against fungal infection

M.A. Hanson[1*], L.B. Cohen[2], A. Marra[1], I. Iatsenko[1,3], S.A. Wasserman[2], and B. Lemaitre[1]

1 Global Health Institute, School of Life Science, École Polytechnique Fédérale de Lausanne (EPFL), Lausanne, Switzerland.
2 Division of Biological Sciences, University of California San Diego (UCSD), La Jolla, California, United States of America.
3 Max Planck Institute for Infection Biology, 10117, Berlin, Germany.
* Corresponding author: M.A. Hanson (mark.hanson@epfl.ch), B. Lemaitre (bruno.lemaitre@epfl.ch)

ORCID IDs:
Hanson: https://orcid.org/0000-0002-6125-3672
Cohen: https://orcid.org/0000-0002-6366-570X
Iatsenko: https://orcid.org/0000-0002-9249-8998
Wasserman: https://orcid.org/0000-0003-1680-3011
Lemaitre: https://orcid.org/0000-0001-7970-1667

Abstract (212 words)

The fruit fly *Drososphila melanogaster* combats microbial infection by producing a battery of effector peptides that are secreted into the haemolymph. The existence of many effectors that redundantly contribute to host defense has hampered their functional characterization. As a consequence, the logic underlying the role of immune effectors is only poorly defined, and exactly how each gene contributes to survival is not well characterized. Here we describe a novel *Drosophila* antifungal peptide gene that we name *Baramicin A*. We show that *BaraA* encodes a precursor protein cleaved into multiple peptides via furin cleavage sites. *BaraA* is strongly immune-induced in the fat body downstream of the Toll pathway, but also exhibits expression in the nervous system. Importantly, we show that flies lacking *BaraA* are viable but susceptible to a subset of filamentous fungi. Consistent with *BaraA* being directly antimicrobial, overexpression of *BaraA* promotes resistance to fungi and the IM10-like peptides produced by *BaraA* synergistically

inhibit growth of fungi in vitro when combined with a membrane-disrupting antifungal. Surprisingly, *BaraA* males but not females display an erect wing phenotype upon infection, pointing a protective role of *BaraA* on the wing muscle or the nervous system. Collectively, we identify a new antifungal immune effector downstream of Toll signalling, improving our knowledge of the *Drosophila* antimicrobial response.

Significance statement

Antimicrobial peptides (AMPs) of the innate immune system provide a front line of defence against infection. Recently AMPs have been implicated in physiological processes including inflammation, aging, and neurodegeneration. *Drosophila melanogaster* has been a useful model for understanding AMP functions and specificities in vivo. Here we describe a new *Drosophila* AMP family, *Baramicin*, which protects flies against fungal infection. The *Baramicin* polypeptide structure is also unique amongst animal AMPs, encoding multiple peptides on a single protein precursor cleaved by furin. Furthermore *Baramicin* mutants display a behavioural response to infection, suggesting Baramicin AMPs interact with more than just pathogens. *Baramicin* adds to our knowledge of the potent *Drosophila* antifungal response, and to growing observations of AMPs acting in seemingly non-canonical roles.

Introduction (806 words)

The innate immune response provides the first line of defence against pathogenic infection. This reaction is usually divided into three stages: i) the recognition of pathogens through dedicated pattern recognition receptors, ii) the activation of conserved immune signalling pathways and iii) the production of immune effectors that target invading pathogens [1,2]. The study of invertebrate immune systems has led to key observations of broad relevance, such as the discovery of phagocytosis [3], antimicrobial peptides (AMPs) [4], and the implication of Toll receptors in metazoan immunity[5]. Elucidating immune mechanisms, genes, and signalling pathways has greatly benefited from investigations in the fruit fly *Drosophila melanogaster*, which boasts a large suite of molecular and genetic tools for manipulating the system. One of the best-characterized immune reactions of *Drosophila* is the systemic immune response.

72 This reaction involves the fat body (an analog of the mammalian liver) producing
73 immune effectors that are secreted into the haemolymph. In *Drosophila*, two NF-κB
74 signalling pathways, the Toll and Imd pathways, regulate most inducible immune
75 effectors: the Toll pathway is predominantly activated in response to infection by
76 Gram-positive bacteria and fungi [5,6], while the immune-deficiency pathway (Imd)
77 responds to the DAP-type peptidoglycan most commonly found in Gram-negative
78 bacteria and a subset of Gram-positive bacteria [7]. These two signalling pathways
79 regulate a transcriptional program that results in the massive synthesis and
80 secretion of humoral effector peptides [6,8]. Accordingly, mutations affecting the
81 Toll and Imd pathways cause extreme susceptibilities to systemic infection that
82 reflect the important contribution of these pathways to host defence. The best-
83 characterized immune effectors downstream of these pathways are antimicrobial
84 peptides (AMPs). AMPS are small and often cationic peptides that disrupt the
85 membranes of microbes, although some have more specific mechanisms [9].
86 Multiple AMP genes belonging to seven well-characterized families are induced
87 upon systemic infection [10]. However transcriptomic analyses have revealed that
88 the systemic immune response encompasses far more than just the canonical AMPs.
89 Many uncharacterized genes encoding small secreted peptides are induced to high
90 levels downstream of the Toll and Imd pathways, pointing to the role for these
91 peptides as immune effectors [11]. In parallel, MALDI-TOF analyses of the
92 haemolymph of infected flies revealed the induction of 24 peaks - mostly
93 corresponding to uncharacterized peptides - that were named "IMs" for Immune-
94 induced Molecules (IM1-IM24) [8]. Many of the genes that encode these components
95 of the immune peptidic secretome have remained largely unexplored. This is mainly
96 due to the fact that these IMs belong to large gene families of small-sized genes that
97 were until recently difficult to disrupt by mutagenesis.
98
99 The CRISPR/Cas9 gene editing approach now allows the necessary precision
100 to delete small genes, singly or in groups, providing the opportunity to dissect
101 effector peptide functions. In 2015 a family of 12 related IM-encoding genes, unified
102 under the name *Bomanins*, were shown to function downstream of Toll. Importantly,

103 a deletion removing 10 out of the 12 Bomanins revealed their potent contribution to
104 defence against both Gram-positive bacteria and fungi [12]. While Bomanins
105 contribute significantly to Toll-mediated defence, their molecular functions are still
106 unknown and it is unclear if they are directly antimicrobial [13]. Two other IMs
107 encoding IM4 and IM14 (renamed *Daisho1* and *Daisho2*, respectively) were shown
108 to contribute downstream of Toll to resistance against specific fungi. Interestingly,
109 Daisho peptides bind to fungal hyphae, suggesting direct antifungal activity [14].
110 Finally a systematic knock-out analysis of *Drosophila* AMPs revealed that they play
111 an important role in defence against Gram-negative bacteria and some fungi, but
112 surprisingly little against Gram-positive bacteria [15]. An unforeseen finding from
113 these recent studies is the high degree of AMP-pathogen specificity: this is perhaps
114 best illustrated by the specific requirement for *Diptericin*, but not other AMPs, in
115 defence against *Providencia rettgeri* [15,16]. Collectively, these studies in *Drosophila*
116 reveal that immune effectors can be broad or specific in mediating host-pathogen
117 interactions. Understanding the logic of the *Drosophila* effector response will thus
118 require a careful dissection of the remaining uncharacterized IMs.
119
120 Previous studies identified an uncharacterized Toll-regulated gene called
121 *IMPPP/CG33470*, which we rename "*BaraA*" (see below), that encodes several IMs,
122 indicating a role in the humoral response. Here, we have improved the annotation of
123 IMs produced by *BaraA* to include: IM10, IM12 (and its sub-peptide IM6), IM13 (and
124 its sub-peptides IM5 and IM8), IM22, and IM24. Using a *BaraA* reporter, we show
125 that *BaraA* is not only immune-induced in the fat body, but also highly expressed in
126 the nervous system. Importantly, we show that flies lacking *BaraA* are viable but
127 susceptible to specific infections, notably by the entomopathogenic fungus
128 *Beauveria bassiana*. Consistent with this, the IM10-like peptides produced by *BaraA*
129 inhibit fungal growth in vitro when combined with the antifungal Pimaricin.
130 Surprisingly, *BaraA* deficient males also display a striking erect wing behaviour
131 upon infection. Collectively, we identify a new antifungal immune effector
132 downstream of Toll signalling, improving our knowledge of the *Drosophila*
133 antimicrobial response.

Results (2923 words):

BaraA is regulated by the Toll pathway

Previous microarray studies from De Gregorio et al. [11] suggest that *BaraA* is primarily regulated by the Toll pathway, with a minor input from the Imd pathway (**Fig.** 1A and **Fig.** S1A-F). Consistent with this, we found several putative NF-κB binding sites upstream of the *BaraA* gene (guided by previous reports [17–19]). Notably there are two putative binding sites for Relish, the transcription factor of the Imd pathway and three putative binding sites for the Dif/Dorsal transcription factors acting downstream of Toll (**Fig.** S1G). We challenged wild-type flies and Imd or Toll pathway mutants (Rel^{E20} and spz^{rm7} respectively) with the Gram-negative bacterium *Escherichia coli*, the yeast *Candida albicans*, or the Gram-positive bacterium *Micrococcus luteus*. RT-qPCR analysis confirms that *BaraA* is induced by infection with *E. coli*, *C. albicans*, or *M. luteus (***Fig.** 1B and **Fig.** S1H). *BaraA* remains highly inducible in a *Relish* mutant background, albeit at slightly reduced level compared to the wild-type. However *BaraA* expression is abolished in spz^{rm7} flies. Collectively, the expression pattern of *BaraA* is reminiscent of the antifungal peptide gene *Drosomycin* with a primary input by the Toll pathway and a minor input from the Imd pathway [10,20].

To further characterize the expression of *BaraA*, we generated a *BaraA-Gal4* transgene in which 1675bp of the *BaraA* promoter sequence is fused to the yeast transcription factor Gal4. Use of *BaraA-Gal4>UAS-mCD8-GFP* (referred to as *BaraA>mGFP*) reveals that *BaraA* is strongly induced in the fat body 60h post infection by *M. luteus* (**Fig.** 1C), but less so by *E. coli* pricking (**Fig.** S1I); dissections confirmed this GFP signal is produced by the fat body. Larvae pricked with *M. luteus* also show a robust GFP signal primarily stemming from the fat body when examined 2hpi (**Fig.** 1D). We also observed a strong constitutive GFP signal in the headcase of

164 adults (**Fig.** 1E), including the border of the eyes and the ocelli (**Fig.** 1F). Dissection
165 confirmed that the *BaraA* reporter is expressed in brain tissue, notably in the central
166 ventral brain furrow. Other consistent signals include GFP in the wing veins and
167 subcutaneously along borders of thoracic pleura in adults (**Fig.** 1G-H), and in
168 spermatheca of females (**Fig.** S1J). There was also sporadic GFP signal in other
169 tissues that included the larval hindgut, the dorsal abdomen of developing pupae,
170 and the seminal vesicle of males.

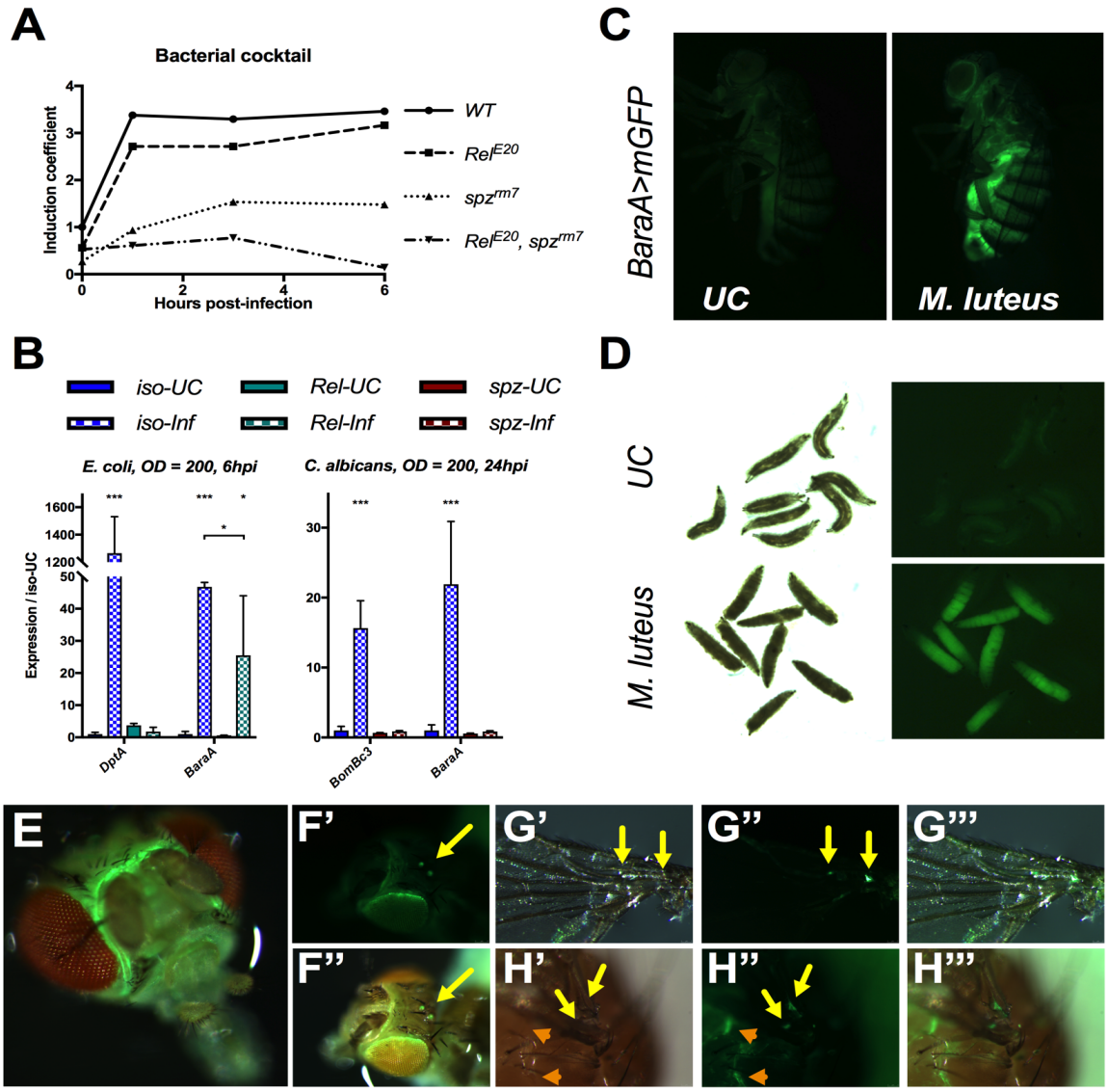

Figure 1: *BaraA* is an immune-induced gene regulated by the Toll pathway. **A)** Expression profile of *BaraA* upon bacterial challenge by a mix of *E. coli* and *M. luteus* (values from De Gregorio *et al.* [1]). *spz^{rm7}* flies lacking Toll signalling have severely reduced *BaraA* expression, and *BaraA* induction is totally abolished in *Rel^{E20}, spz^{rm7}* double mutants. **B)** *BaraA* expression profiles in wild-type, *spz^{rm7}* and *Rel^{E20}* flies upon septic injury with the Gram-negative bacterium *E. coli* and the yeast *C. albicans*. *DptA* and *BomBc3* were used as inducible control genes for the Imd and Toll pathways respectively. Floating asterisks indicate significance relative to *iso-UC* where: * = p < .05 and, *** = p < .001. **C-D)** Use of a *BaraA* reporter (*BaraA-Gal4;* UAS-m*CD8-GFP* referred to as *BaraA>mGFP*) reveals that *BaraA* is induced upon infection in the fat body of adults **(C)** and in larvae **(D)**. Representative images taken 60h (adults) or 2h (larvae) after handling alone (UC) or infection with *M. luteus* (OD=200). E-H) *BaraA>mGFP* is highly expressed in the head and central nervous system **(E)**, behind the eyes and in the ocelli **(F)**, in the wing veins **(G-H** yellow arrows**)**, and beneath the cuticle in the thorax **(H**, orange arrows**)**.

171

172 ***Baramicin A encodes a precursor protein cleaved into multiple peptides***

173

174 Previous studies using bioinformatics and proteomics have suggested that
175 four highly immune-induced peptides (IM10, IM12, IM13, and IM24) are encoded in
176 tandem as a single polypeptide precursor by *IMPPP/BaraA* [8,21]. Some less-
177 abundant sub-peptides (IM5, IM6, and IM8) are also produced by additional
178 cleavage of IM12 and IM13 [21]. Using a newly generated null mutant ("*ΔBaraA,*"
179 described below), we analyzed haemolymph samples of infected wild-type and
180 *ΔBara* flies by MALDI-TOF analysis. We confirmed the loss of the seven immune-
181 induced peaks corresponding to IMs 5, 6, 8, 10, 12, 13, and 24 in *ΔBaraA* flies (**Fig.**
182 2A). We also noticed that an additional immune-induced peak at ~5975 Da was
183 absent in our *BaraA* mutants. Upon re-visiting the original studies that annotated
184 the *Drosophila* IMs, we realized this peak corresponded to IM22, whose sequence
185 was never determined [8,21] (see supplementary information for details). We
186 subjected immune-induced haemolymph to LC-MS proteomic analysis following
187 trypsin digestion and found that in addition to the known IMs of *BaraA* (IMs 5, 6, 8,
188 10, 12, 13, and 24), trypsin-digested fragments of the *BaraA* C-terminus peptide
189 were also detectable in the haemolymph (**Fig.** S2). The range of detected fragments
190 did not match the full length of the C-terminus exactly, as the first four residues
191 were absent in our LC-MS data (a truncation not predicted to arise via trypsin
192 cleavage). The *BaraA* C-terminus lacking these four residues has a calculated mass
193 of 5974.5 Da, exactly matching the observed mass of the IM22 peak absent in *BaraA*
194 mutant flies. Furthermore in other *Drosophila* species these four residues of the
195 *BaraA* C-terminus are an RXRR furin cleavage motif (**Fig.** S3A). IM22 cleavage via
196 this motif should produce the same IM22 domain as seen in *D. melanogaster*. Taken
197 together, we conclude that IM22 is the mature form of the BaraA protein C-
198 terminus.

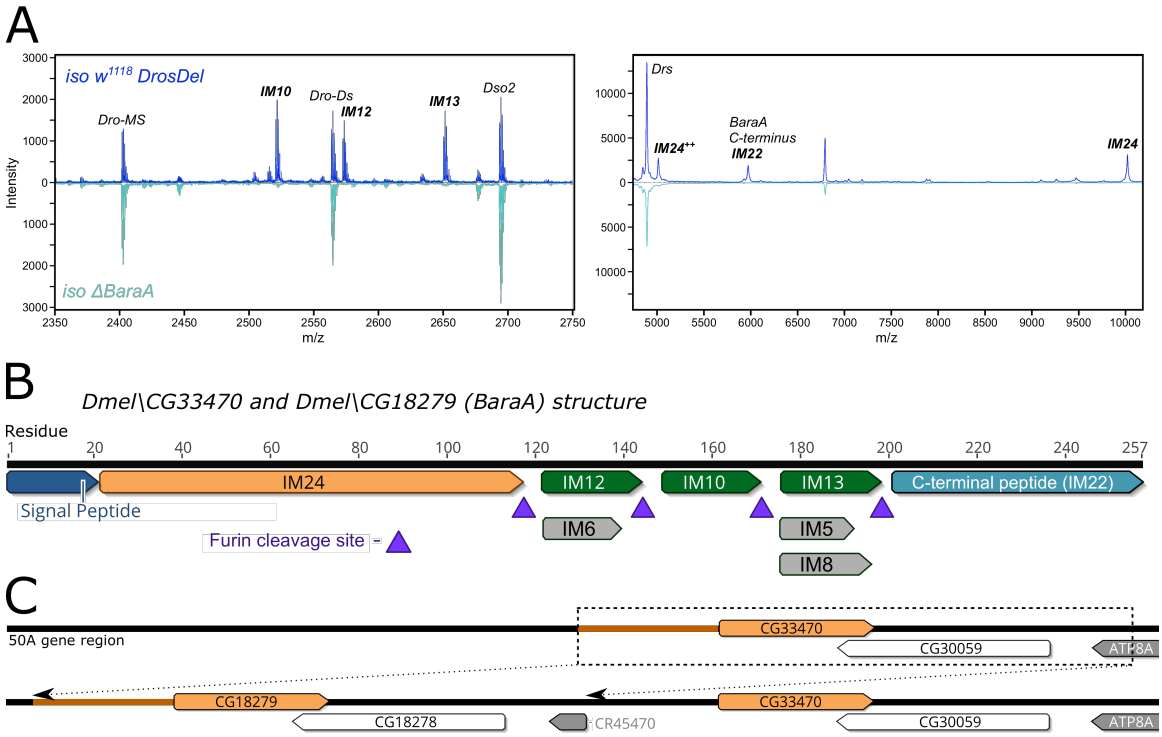

Figure 2: The *Baramicin A* polypeptide genes. A) MALDI-TOF analysis of haemolymph from *iso w*^{1118} wild-type and *iso ΔBaraA* flies 24 hours post-infection (hpi) confirms that *BaraA* mutants fail to produce the IM10-like and IM24 peptides. *iso ΔBaraA* flies also fail to produce an immune-induced peak at ~5794 Da corresponding to IM22 (the C-terminal peptide of BaraA, see supplementary information). **B)** The *BaraA* gene encodes a precursor protein that is cleaved into multiple mature peptides at RXRR furin cleavage sites. The sub-peptides IMs 5, 6, and 8 are additional minor cleavage products of IM12 and IM13. **C)** There is a *BaraA* locus duplication event present in the Dmel_R6 reference genome. This duplication is not fixed in laboratory stocks and wild-type flies (Hanson and Lemaitre, 2020; in prep.).

Thus, a single gene, *BaraA*, contributes to one third of the originally described IMs. These peptides are encoded as a polypeptide precursor interspersed by furin cleavage sites (e.g. RXRR) (**Fig.** 2B). We note that the IM10, IM12 and IM13 peptides are tandem repeats of related peptides, which we collectively refer to as "IM10-like" peptides (**Fig.** S3B). The IM22 peptide also contains a similar motif as the IM10-like peptides (**Fig.** S3A-B), suggesting a related biological activity. We rename this gene "*Baramicin A*" (symbol: *BaraA*) for the Japanese idiom Bara Bara (

220 バラバラ), meaning “to break apart;” a reference to the fragmenting structure of the
221 *Baramicin* precursor protein and its many peptidic products.
222
223 ***A BaraA duplication is present in several laboratory stocks***
224
225 Over the course of our investigation, we realized that *IMPPP (CG18279)* was
226 identical to its neighbour gene *CG33470* owing to a duplication event of the *BaraA*
227 locus present in the *D. melanogaster* reference genome. The exact nature of this
228 duplication, and its consequence on the immune response is discussed in a separate
229 article (Hanson and Lemaitre; in prep). In brief, the duplication involves the entire
230 *BaraA* gene including over 1kbp of 100% identical promoter sequence, and also the
231 neighbouring sulfatase gene CG30059 and the 3’ terminus of the *ATP8A* gene region
232 (**Fig.** 2C). We distinguish the two daughter genes as *BaraA1 (CG33470)* and *BaraA2*
233 *(CG18279).* Available sequence data suggests the *BaraA1* and *BaraA2* transcripts are
234 100% identical. Interestingly, *BaraA* copy number is variable in common lab strains
235 and wild flies, indicating this duplication event is not fixed in *D. melanogaster*
236 (Hanson and Lemaitre; in prep).
237
238 ***Over-expression of BaraA improves the resistance of immune deficient flies***
239
240 *Imd, Toll* deficient flies are extremely susceptible to microbial infection as
241 they fail to induce hundreds of immune genes, including antimicrobial peptides [11].
242 It has been shown that over-expression of even a single AMP can improve the
243 resistance of *Imd, Toll* deficient flies [22]. As such, immune gene over-expression in
244 *Imd, Toll* immune-compromised flies provides a sensitive assay for testing the
245 ability of a gene to contribute to defence independent of other immune effectors. We
246 applied this strategy to *Baramicin A* by generating flies that constitutively express
247 *BaraA* using the ubiquitous *Actin5C-Gal4* driver in an immune-deficient Rel^{E20}, spz^{rm7}
248 background (**Fig.** 3A). In these experiments, we pooled results from both males and
249 females due to the very low rate of homozygous *Rel, spz* adults, particularly when

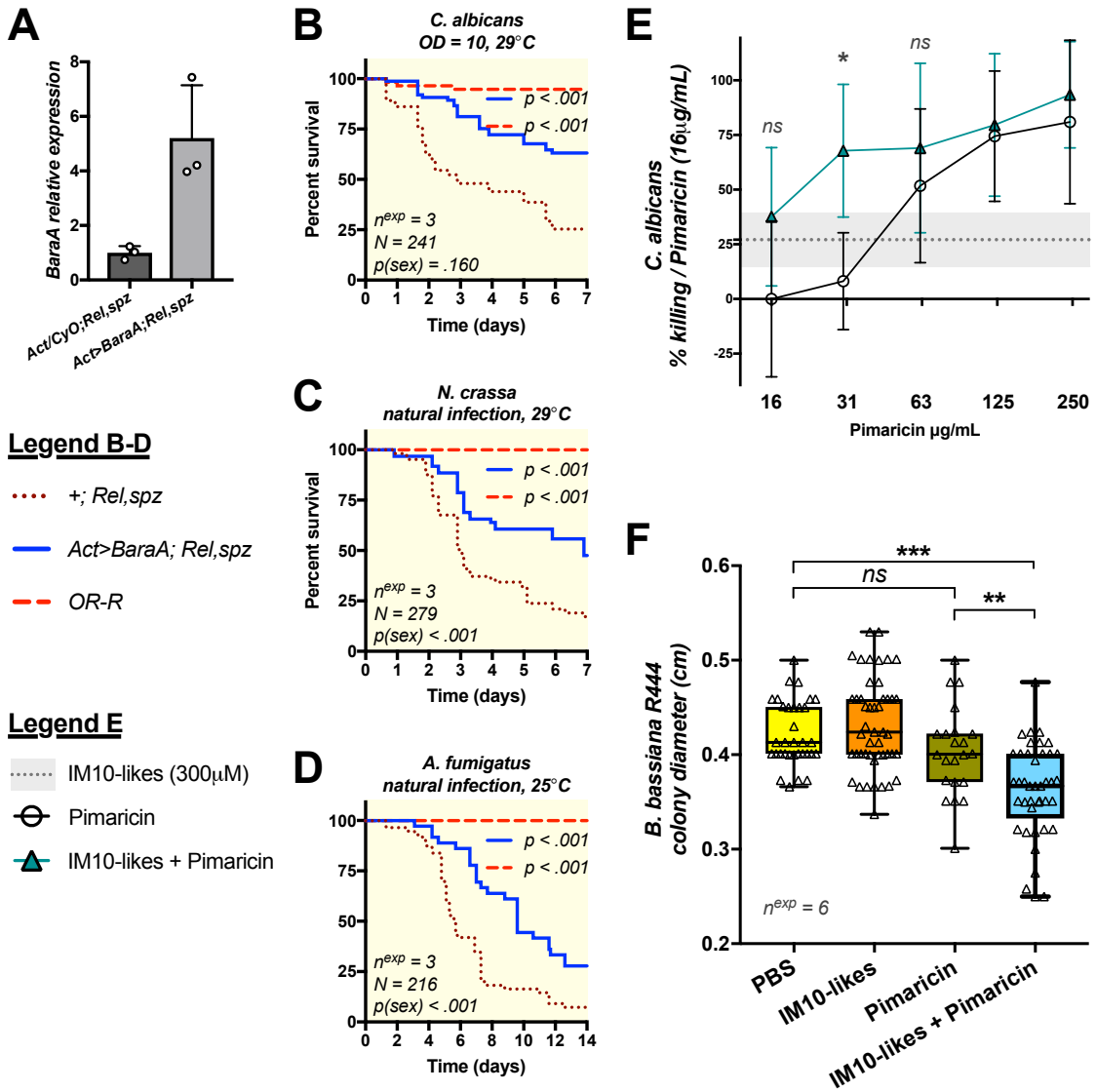

Figure 3: Overexpression of *BaraA* partially rescues the susceptibility of *Rel, spz* flies against fungi and BaraA IM10-like peptides inhibit fungal growth in vitro. A) Validation of the *Act>BaraA* construct in unchallenged flies. **B-D)** Overexpression of *BaraA* (*Act>BaraA)* rescues the susceptibility of *Rel, spz* flies upon systemic infection with *C. albicans* **(B)**, or natural infection with either *N. crassa* or *A. fumigatus* **(C-D)**. Survivals represent pooled results from males and females (see **Fig.** S4 for sex-specific survival curves). **E)** A 300µM cocktail of the three IM10-like peptides improves the killing activity of the antifungal Pimaricin against *C. albicans* yeast. Error bars and the shaded area (IM10-likes alone) represent ±1 standard deviation from the mean. Killing activity (%) was compared against no-peptide controls, then normalized to the activity of Pimaricin alone. **F)** The IM10-like peptide cocktail also synergizes with Pimaricin to inhibit mycelial growth of *B. bassiana strain R444*. The diameters of individual colonies of *B. bassiana* were assessed after four days of growth at 25°C after peptide treatment.

252 combined with *Actin-Gal4*. Similar trends were seen in both sexes, and separate
253 male and female survival curves are shown in **Fig.** S4.
254
255 Ubiquitous *BaraA* expression marginally improved the survival of *Rel, spz*
256 flies upon bacterial infection with *Pectobacterium carotovora (Ecc15)* and to a lesser
257 extent *M luteus* bacteria, while having no effect on *E. coli* (**Fig. S4A-C**). However,
258 ubiquitous expression of *BaraA* provided a more pronounced protective effect
259 against infection by a variety of fungal pathogens. This was true upon pricking with
260 *C. albicans* (**Fig.** 3B), or upon natural infections using *Aspergillus fumigatus* or
261 *Neurospora crassa* filamentous fungi (**Fig.** 3C-D). This over-expression study reveals
262 that *BaraA* alone can partially rescue the susceptibility of *Imd, Toll* deficient flies to
263 infection, and points to a more prominent role for *BaraA* in antifungal defence.
264
265 ***IM10-like peptides display antifungal activity in vitro***
266
267 *The Baramicin A* gene encodes a polypeptide precursor that ultimately
268 produces multiple mature peptides. However the most prominent *BaraA* products
269 are the 23-residue IM10, 12, and 13 peptides (collectively the "IM10-like" peptides);
270 indeed three IM10-like peptides are produced for every one IM24 peptide (**Fig.** 2B),
271 and IM22 also bears an IM10-like motif (**Fig.** S3). This prompted us to explore the in
272 vitro activity of the BaraA IM10-like peptides as potential AMPs.
273
274 We synthesized IM10, IM12, and IM13 and performed in vitro antimicrobial
275 assays with these three IM10-like peptides using a 1:1:1 cocktail with a final
276 concentration of 300μM (100 μM each of IM10, IM12, and IM13). Using a protocol
277 adapted from Wiegand et al. [23], we monitored the microbicidal activity of this
278 peptide cocktail either alone, or in combination with membrane-disrupting
279 antibiotics that facilitate peptide entry into the cell. We based this approach on
280 previous studies that showed e.g. that the microbicidal activities of Abaecin-like
281 peptides, which target the bacterial DNA chaperone *DnaK,* increase exponentially in
282 combination with a membrane disrupting agent [24–26]. We did not detect any

283 killing activity of our IM10-like peptide cocktail alone against *Ecc15, Enterococcus*
284 *faecalis,* or *C. albicans*. We also found no activity of IM10-like peptides against *Ecc15*
285 *or E. faecalis* when co-incubated with a sub-lethal dose of Cecropin or Ampicillin
286 respectively. However, we observed a synergistic interaction between IM10-like
287 peptides and the antifungal Pimaricin against *C. albicans* (**Fig.** 3E). Co-incubation of
288 the IM10-like cocktail with Pimaricin significantly improved the killing activity of
289 Pimaricin at 32μg/mL relative to either treatment alone. While not statistically
290 significant, the combination of IM10-like cocktail and Pimaricin also outperformed
291 either the IM10-like cocktail or Pimaricin alone across the entire range of Pimaricin
292 concentrations tested.
293
294 We next co-incubated preparations of *B. bassiana* R444 spores under the
295 same conditions as used previously with *C. albicans*, plated 2μL droplets, and
296 assessed the diameters of colonies derived from individual spores after 4 days of
297 growth at 25°C. We found that neither the IM10-like cocktail nor Pimaricin alone
298 affected colony diameter relative to PBS buffer control alone (Tukey's HSD: p =
299 0.775 and 0.430 respectively). However in combination, the IM10-like cocktail plus
300 Pimaricin led to significantly reduced colony size compared to either treatment
301 alone (**Fig.** 3F, Tukey's HSD: p = .004). This indicates that incubation with IM10-like
302 peptides and Pimaricin synergistically inhibits *B. bassiana* mycelial growth,
303 revealing an otherwise cryptic antifungal effect of the BaraA IM10-like peptides.
304
305 Overall, we found that IM10-like peptides alone do not kill *C. albicans* yeast
306 or impair *B. bassiana* mycelial growth in vitro. However IM10-like peptides seem to
307 synergize with the antifungal Pimaricin to inhibit growth of both of these fungi.
308
309 ***BaraA deficient flies broadly resist as wild type upon bacterial infection***
310
311 To further characterize *BaraA* function, we generated a null mutation of
312 *BaraA* by replacing the 'entire' *BaraA* locus with a dsRed cassette using CRISPR

313 mediated homology-directed repair in a w^{1118} genetic background that contains only
314 one *BaraA* gene copy. This mutation ($BaraA^{SW1}$ hereafter "*ΔBaraA*") was isogenized
315 by seven rounds of backcrossing into the w^{1118} *DrosDel* isogenic genetic background
316 (*iso* w^{1118}) [27] as described in Ferreira et al. [28]. Relevant to this study, both our
317 *iso* w^{1118} and *OR-R* wild type lines contain the duplication and thus have both *BaraA1*
318 *and A2* genes, while both copies are absent in *ΔBaraA* flies.
319
320 We validated these mutant lines by PCR, qPCR and MALDI-TOF peptidomics
321 (**Fig.** 2A, supplementary data file 1). *BaraA*-deficient flies were viable with no
322 morphological defect. Furthermore, *ΔBaraA* flies have wild-type Toll and Imd
323 signalling responses following infection, indicating that *BaraA* is not required for the
324 activation of these signaling cascades (**Fig.** S5). We next challenged *BaraA* mutant
325 flies using two genetic backgrounds (*w; ΔBaraA* and *iso ΔBaraA*) with a variety of
326 pathogens. We included Imd-deficient Rel^{E20} flies, Toll deficient spz^{rm7} flies and
327 *Bomanin* deficient $Bom^{\Delta 55C}$ flies as positive controls. We observed that *BaraA* null
328 flies have comparable resistance as wild type to infection with the Gram-negative
329 bacteria *Ecc15* or *Providencia burhodogranariea* (**Fig.** S6A-B), or with the Gram-
330 positive bacterium *B. subtilis* (**Fig.** S6C). In contrast, we saw a mild increase in the
331 susceptibility of *w; ΔBaraA* flies to infection by the Gram-positive bacterium *E.*
332 *faecalis* (HR = +0.73, p = .014), which was consistent in *iso ΔBaraA* flies, although
333 this was not statistically significant (**Fig.** 4A). This mild susceptibility was also
334 observed using flies carrying the *BaraA* mutation over a deficiency
335 (*ΔBaraA/Df(BaraA))*, as well as in flies ubiquitously expressing *BaraA* RNAi (**Fig.**
336 S7); however none of these sets of survival experiments individually reached
337 statistical significance.
338
339 ***BaraA mutant flies are highly susceptible to fungal infection***
340
341 Entomopathogenic fungi such as *Beauveria bassiana* represent an important
342 class of insect pathogens [6]. They have the ability to directly invade the body cavity

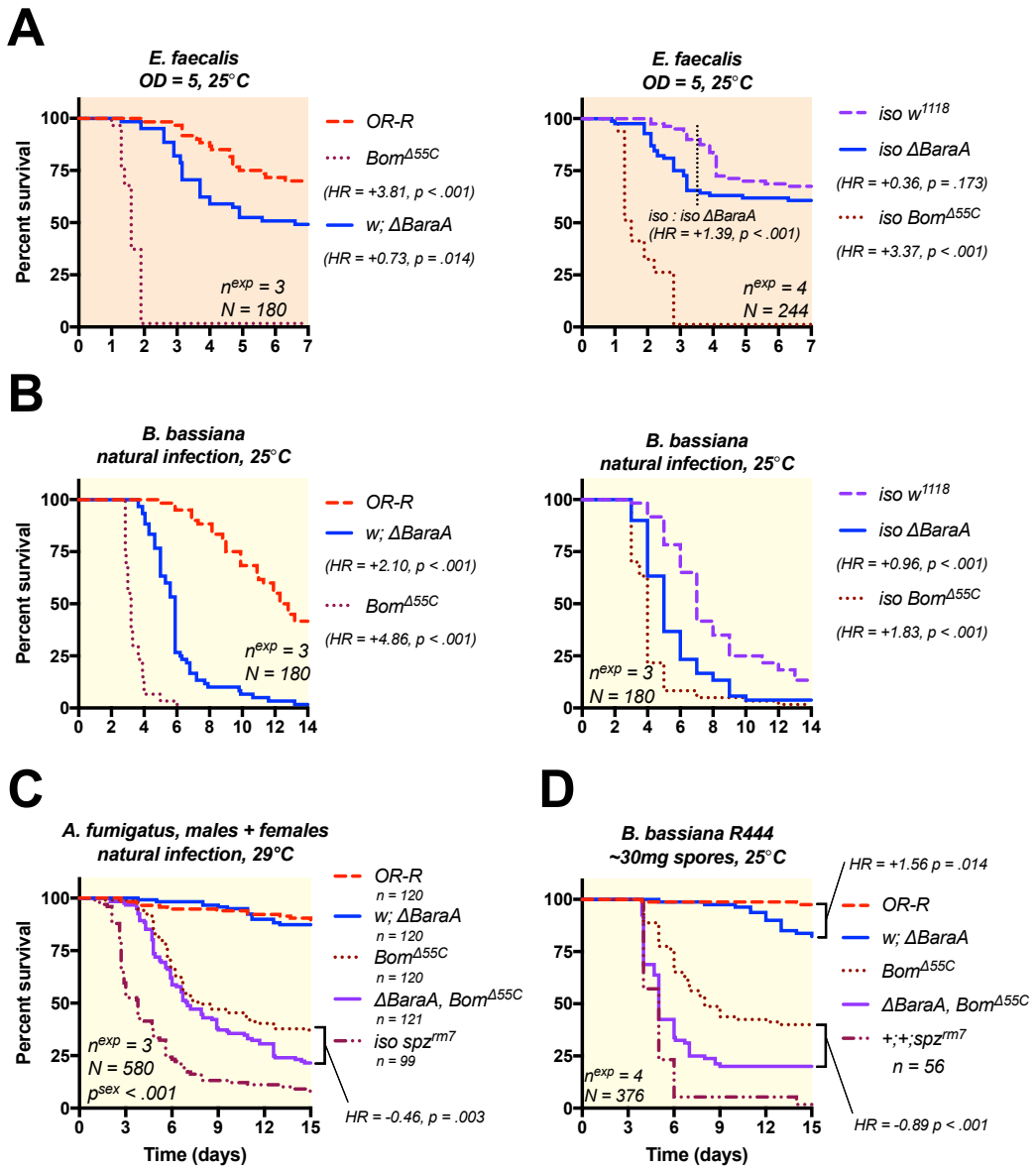

Figure 4: *ΔBaraA* flies are most susceptible to fungal infection. A) *BaraA* mutants with two different genetic backgrounds (here called *w* or *iso*) display a mild susceptibility to systemic infection with *E. faecalis*. This presents as an earlier mortality in the *iso* background (dotted line). However, survival in *iso ΔBaraA* flies was not significantly different from wild type at seven days post-infection (p = .173). **B)** *BaraA* mutants are susceptible to natural infection with the entomopathogenic fungus *B. bassiana*. **C-D)** *ΔBaraA* , $Bom^{\Delta 55C}$ double mutant flies were more susceptible to natural infection with *A. fumigatus* **(C)** and *B. bassiana R444* **(D)** than $Bom^{\Delta 55C}$ single mutant flies (also see **Fig.** S6E-F).

353 by crossing through the insect cuticle. The Toll pathway is critical to survive fungal
354 pathogens as it is directly responsible for the expression of *Bomanins*, *Daishos*,
355 *Drosomycin* and *Metchnikowin* antifungal effectors [12,14,15,29,30]. The fact that i)
356 *BaraA* is Toll-regulated, ii) BaraA IM10-like peptides have antifungal properties in
357 vitro , and iii) *BaraA* overexpression improves the resistance of *Imd, Toll* deficient
358 flies against fungi all point to a role for *BaraA* against fungal pathogens.
359
360 We infected *BaraA* mutants and wild-type flies by rolling flies in sporulating
361 *B. bassiana* petri dishes. Strikingly, both *w; ΔBaraA* and *iso ΔBaraA* flies displayed a
362 pronounced susceptibility to natural infection with *B. bassiana* (HR = +2.10 or +0.96
363 respectively, p < .001 for both) (**Fig.** 4B). An increased susceptibility to fungi was
364 also observed using flies carrying the *BaraA* mutation over a deficiency (**Fig.** S8A) or
365 that ubiquitously express *BaraA* RNAi (**Fig.** S8B). Moreover, constitutive *BaraA*
366 expression (*Act-Gal4>UAS-BaraA)* in an otherwise wild-type background improves
367 survival to *B. bassiana* relative to *Act-Gal4>OR-R* controls (HR = -0.52, p = .010) (**Fig.**
368 S8C).
369
370 In contrast to the findings with *B. bassiana*, survival analysis revealed only a
371 minor susceptibility of *BaraA* mutants upon infection via injury with *C. albicans* or
372 natural infection with *A. fumigatus* (**Fig.** S6D-F), neither of which reached statistical
373 significance. Collectively, our survival analysis points most strongly to a role for
374 *BaraA* in defence against the entomopathogenic fungus *B. bassiana*.
375
376 ***BaraA contributes to antifungal defence independent of Bomanins***
377
378 Use of compound mutants carrying multiple mutations in effector genes has
379 shown that some of them additively contribute to host resistance to infection. For
380 instance, *Drosomycin, Metchnikowin* double mutants are more susceptible than
381 single mutants to *C. albicans* [15]. Compound deletions of immune genes can also
382 reveal contributions of immune effectors that are not detectable via single mutant
383 analysis [31,32]. Recent studies have indicated that *Bomanins* play a major role in

384 defence against fungi [12,13], though their mechanism of action is unknown. This
385 prompted us to investigate the interaction of *Bomanins* and *BaraA* in defence against
386 fungi. To do this, we recombined the $Bom^{\Delta 55C}$ mutation (that removes a cluster of 10
387 *Bomanin* genes) with *ΔBaraA.* These *w; ΔBaraA,* $Bom^{\Delta 55C}$ double mutant flies were
388 perfectly viable. While natural infection with *Aspergillus fumigatus* did not induce
389 significant mortality in *BaraA* single mutants, we observed that the combined
390 *ΔBaraA* and $Bom^{\Delta 55C}$ mutations increases fly susceptibility to this pathogen relative
391 to $Bom^{\Delta 55C}$ alone (HR = -0.46, p = .003; **Fig.** 4C).
392
393 We next exposed these *ΔBaraA*, $Bom^{\Delta 55C}$, double mutant flies to 30mg of
394 commercial spores of *B. bassiana R444*, which we found to be a less virulent
395 infection model. This is equivalent to approximately 60 million spores, much of
396 which are removed afterwards upon fly grooming. When using this infection
397 method, we found that *BaraA* mutation markedly increases the susceptibility of *Bom*
398 mutant flies (HR = -0.89, p < .001), approaching spz^{rm7} susceptibility (**Fig.** 4D).
399
400 We conclude that the contribution of *BaraA* to defence does not rely on the
401 presence of *Bomanins*, and vice versa. This finding is consistent with the ability of
402 constitutively expressed *BaraA* to improve survival outcome even in *Imd, Toll*
403 deficient flies. Taken together, these results suggest *BaraA* improves survival
404 against fungi independent of other effectors of the systemic immune response,
405 consistent with a direct effect on invading fungi.
406
407 ***ΔBaraA males display an erect wing phenotype upon infection***
408
409 While performing infections with *A. fumigatus*, we observed a high
410 prevalence of *BaraA* mutant flies with upright wings (**Fig. 5**A-B), a phenotype
411 similar to the effect of disrupting the gene encoding the "*erect wing"* (*ewg*)
412 transcription factor [33]. Curiously, this erect wing phenotype was most specifically
413 observed in males. Upon further observation, erect wing was observed not only
414 upon *A. fumigatus* infection, but also upon infections with all Gram-positive bacteria

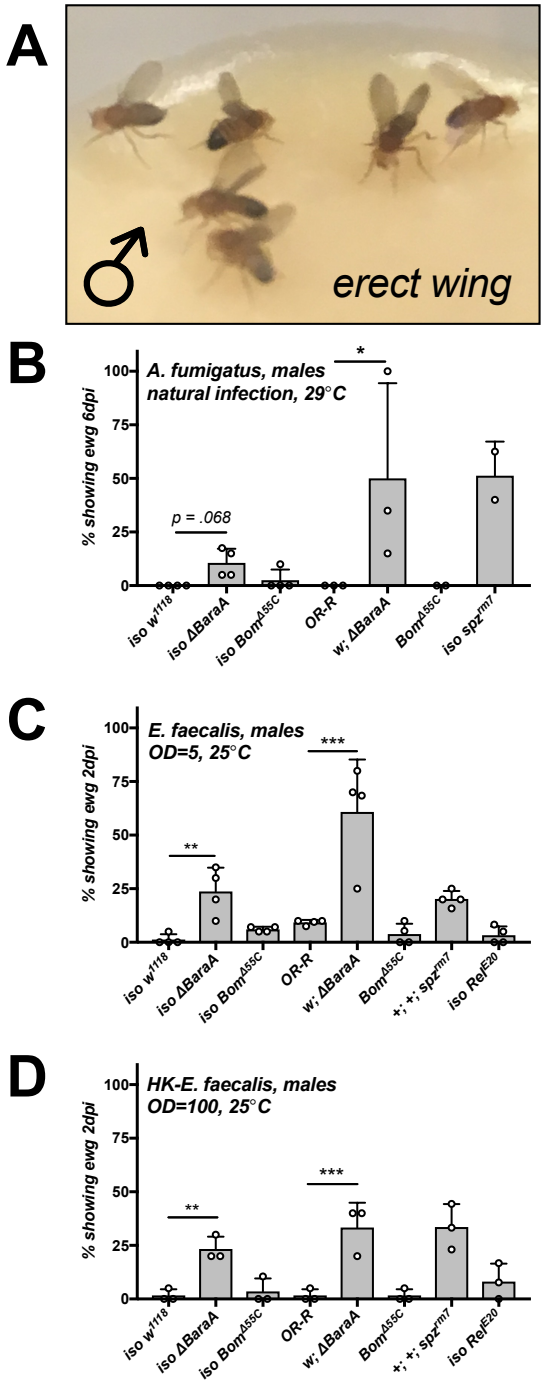

and fungi tested (**Table S1**). Increased prevalence of erect wing flies was observed upon infection with both live (**Fig.** 5C) and heat-killed *E. faecalis* (**Fig.** 5D), but less so upon clean injury or via infection with the Gram-negative bacteria *Ecc15*. (**Fig. S9**A-B). Thus, the erect wing phenotype appears to be observed in *BaraA* mutants in response to stimuli known to activate the Toll pathway, but does not require a live infection.

Such a phenotype in infected males has never been reported, but is reminiscent of the wing extension behaviour of flies infected by the brain-controlling "zombie" fungus *Enthomopthera muscae* [34]. Intrigued by this phenotype, we further explored its prevalence in other genetic backgrounds. We next confirmed that this phenotype was also observed in other *BaraA*-deficient backgrounds such as *Df(BaraA)/ΔBara*; however the penetrance was variable from one

Figure 5: *ΔBaraA* males display an erect wing phenotype upon infection. A) *ΔBaraA* males displaying erect wing six days after *A. fumigatus* natural infection. B-D) spz^{rm7} and *ΔBaraA* males, but not $Bom^{\Delta 55C}$ or Rel^{E20} flies display the erect wing phenotype upon natural infection with *A. fumigatus* **(B)**, or septic injury with live **(C)** or heat-killed *E. faecalis* **(D)**. Barplots show the percentage of flies displaying erect wing following treatment, with individual data points reflecting replicate experiments. Additional challenges are shown in Table S1.

440 background to another. Erect wing was also observed in *ΔBaraA*/+ heterozygous
441 flies (*Df(BaraA)/+* or *ΔBaraA*/+), indicating that the lack of one dose of *BaraA* was
442 sufficient to cause the phenotype (**Fig. S9**C and **Table S1**). Moreover, spz^{rm7} flies that
443 lack functional Toll signalling phenocopy *ΔBaraA* flies and display erect wing, but
444 other immune-deficient genotypes such as mutants for the Toll-regulated *Bomanin*
445 effectors ($Bom^{\Delta 55C}$), or Rel^{E20} mutants that lack Imd signalling, do not frequently
446 display erect wing (**Fig. 5**C-D, **Table S1**). Thus the erect wing behaviour is not linked
447 to susceptibility to infection, but rather to loss of *BaraA* upon stimuli triggering the
448 Toll immune pathway. This phenotype suggests an additional effect of *BaraA* on
449 tissues related to the wing muscle or in the nervous system.
450

451 # Discussion (1508 words):

452

453 Seven *Drosophila* AMPs were identified in the 1980's-1990's either by
454 homology with AMPs characterized in other insects or owing to their abundant
455 production and microbicidal activities in vitro [35]. In the 2000s, genome
456 annotations revealed the existence of many additional paralogous genes from the
457 seven well-defined families of AMPs [36,37]. At that time, microarray and MALDI-
458 TOF analyses also revealed the existence of many more small immune-induced
459 peptides, which may function as AMPs [8,21]. Genetic analyses using loss of function
460 mutations have recently shown that some of these peptides do play an important
461 role in host defence, however key points surrounding their direct microbicidal
462 activities remain unclear. In 2015, *Bomanins* were shown to be critical to host
463 defence using genetic approaches, but to date no activity in vitro has been found
464 [12,13]. Two candidate AMPs, Listericin [38] and GNBP-like3 [39], were shown to
465 inhibit microbial growth upon heterologous expression using S2 cell lines or
466 bacteria respectively. Most recently, Daisho peptides were shown to bind to fungal
467 hyphae ex vivo, and are required for resisting fungal infection in vivo [14]. However
468 the mechanism and direct microbicidal activity of these peptides at physiological
469 concentrations was not assessed.

470

471 In this study, we provide evidence from four separate experimental
472 approaches that support adding *BaraA* to the list of bona-fide antifungal peptides.
473 First, the *BaraA* gene is strongly induced in the fat body upon infection resulting in
474 abundant peptide production. *BaraA* is also tightly regulated by the Toll pathway,
475 which orchestrates the antifungal response. Second, loss of function study shows
476 that *BaraA* contributes to resistance against various fungi. Our in vivo analyses
477 reveal a potential range of activity for *BaraA* in defence against the yeast *C. albicans*,
478 the mould *A. fumigatus*, and most prominently the entomopathogenic fungus *B.*
479 *bassiana*; a marginal effect was also seen upon *E. faecalis* bacterial infections. Third,
480 the antifungal activity of *BaraA* is independent of other key effectors. Over-
481 expression of *BaraA* in the absence of other inducible peptides increased resistance
482 of *Imd, Toll* deficient flies to *C. albicans*, *A. fumigatus*, and *N. crassa*. Moreover *BaraA,*
483 *Bomanin* double mutants suffered greater susceptibility than *Bomanin* mutants
484 alone even against otherwise avirulent fungal pathogens. Lastly, in vitro assays
485 show that a cocktail of the *BaraA* IM10-like peptides possess antifungal activity
486 when co-incubated with the membrane disrupting antifungal Pimaricin.
487

488 While it is difficult to estimate the concentration of BaraA peptides in the
489 haemolymph of infected flies, it is expected based on MALDI-TOF peak intensities
490 that the IM10-like peptides should reach concentrations similar to other AMPs (up
491 to 100μM) [10,20]; Our in vitro assays used a peptide cocktail at the upper limit of
492 this range. AMPs are often - but not exclusively – positively charged. This positive
493 charge is thought to recruit these molecules to negatively charged membranes of
494 microbes [10]. However the net charges at pH=7 of the IM10-like peptides are: IM10
495 +1.1, IM12 +0.1, and IM13 -0.9. Given this range of net charge, IM10-like peptides
496 are not overtly cationic. However some AMPs are antimicrobial without being
497 positively charged, exemplified by human Dermicidin [40] and anionic peptides of
498 Lepidoptera that also synergize with membrane-disrupting agents [41]. However
499 more extensive in vitro experiments with additional fungi should confirm the range

500 of BaraA peptide activities, and assay the potential activities of IM22 and IM24,
501 which were not included in this study.
502
503 Entomopathogenic fungi pose a ubiquitous challenge to insects, and in turn
504 insects use a combination of mechanisms to combat invading fungi. This defence
505 relies largely on humoral factors most notably melanization and the production of
506 host defence peptides. In *Drosophila*, five classes of host defence peptides (plus
507 isoforms) have been shown to contribute to survival against fungi: Drosomycin,
508 Metchnikowin, Bomanins, Daishos, and now the Baramicin A peptides. Additional
509 uncharacterized peptides regulated by the Toll pathway could expand this list
510 further. It interesting to note that *Baramicin* is found conserved throughout the
511 *Drosophila* genus and in closely related outgroup species (Hanson and Lemaitre; in
512 prep) with a species range similar to *Metchnikowin* and *Daisho*. Meanwhile the most
513 well studied antifungal peptide Drosomycin is in fact specific only to *D.*
514 *melanogaster* and close relatives. While other AMPs such as the antibacterial
515 peptides Attacin, Cecropin, and Defensin, are conserved across Diptera and other
516 insect orders, antifungal peptide genes found in *Drosophila* appear to be younger
517 [14,42]. The presence of these seemingly novel antifungal genes could be one factor
518 that allows *Drosophila* species to exploit such a wide variety of microbe-infested
519 niches compared to more ecologically restricted insect lineages.
520
521 Our study also reveals that the *Baramicin A* gene alone produces at least 1/3
522 of the initially reported IMs. In addition to the IM10-like peptides and IM24 that
523 were previously assigned to *BaraA* [21], we show IM22 is encoded by the C terminus
524 of *BaraA*, and is conserved in other *Drosophila* species. The production of multiple
525 IMs encoded as tandem repeats between furin cleavage sites is built-in to the BaraA
526 protein design akin to a "protein operon." Such tandem repeat organization is rare,
527 but not totally unique among AMPs. This structure was first described in the
528 bumblebee AMP Apidaecin [43], and has since also been found in Drosocin of
529 *Drosophila neotestacea* [44]. In *D. melanogaster*, several AMPs including Attacin C
530 and its pro-peptide MPAC are also furin-processed, and both parts synergize in

531 killing bacteria [24]. Therefore furin cleavage in Attacin C enables the precise co-
532 expression of distinct peptides with synergistic activity. It is interesting to note that
533 IM10-like peptides did not show antifungal activity in the absence of membrane
534 disruption by Pimaricin. An attractive hypothesis is that longer peptides encoded by
535 BaraA such as IM22 and IM24 could contribute to the antifungal activity of *BaraA* by
536 membrane permeabilization, allowing the internalization of IM10-like peptides. Of
537 note: the IM24 domain is also encoded by two *Baramicin* paralogs named *BaraB* and
538 *BaraC*, which are expressed in the nervous system but do not participate in the
539 inducible immune response (Hanson et al., in prep). This suggests that the IM24
540 peptidic domain can play a role beyond systemic immunity. The BaraA IM24 peptide
541 is a short Glycine-rich peptide (96 AA) that is positively-charged (charge +2.4 at
542 pH=7). These traits are shared by amphipathic membrane-disrupting AMPs such as
543 Attacins, and also neuropeptides that utilize amphipathic domains to accumulate in
544 neuronal membranes [45]. Thus roles for the Baramicin IM24 domain in both
545 immunity and neurology are not mutually exclusive.
546
547 An unexpected observation of our study is the display of an erect wing
548 phenotype by *BaraA* deficient males upon infection. Our study suggests that this is
549 not a consequence of the genetic background, but rather relies on the activation of
550 the Toll pathway in the absence of *BaraA*. The *erect wing* gene, whose inactivation
551 causes a similar phenotype, is a transcription factor that regulates synaptic growth
552 in developing neuromuscular junctions [33]. This raises the intriguing hypothesis
553 that immune processes downstream of the Toll ligand Spaetzle somehow affect wing
554 neuromuscular junctions, and that *BaraA* modulates this activity. Another puzzling
555 observation is the sexual dimorphism exhibited for this response. It should be noted
556 that male courtship and aggression displays involve similar wing extension
557 behaviours. Koganezawa et al. [46] showed that males deficient for *Gustatory*
558 *receptor 32a (Gr32a)* failed to unilaterally extend wings during courtship display.
559 *Gr32a*-expressing cells extend into the subesophageal ganglion where they contact
560 mAL, a male-specific set of interneurons involved in unilateral wing display [46]. As
561 erect wing is male-specific, we speculate this *BaraA*-mediated effect might rely on

562 interactions with such male-specific neurons. *BaraA* is highly produced in the fat
563 body upon infection but also expressed in the nervous system. Further studies
564 should decipher whether the preventative effect of *BaraA* on the erect wing
565 phenotype is cell autonomous or linked to BaraA peptides secreted into the
566 haemolymph. Erect wing is also induced by heat-killed bacteria, and is not observed
567 in *Bomanin* or *Relish* mutants, indicating that the erect wing phenotype is not a
568 generic consequence of susceptibility to infection. Recent studies have highlighted
569 how NF-κB signalling in the brain is activated by bacterial peptidoglycan [47], and
570 that immune effectors expressed either by fat body surrounding the brain or from
571 within brain tissue itself affect memory formation [39]. Moreover, an AMP of
572 nematodes regulates aging-dependent neurodegeneration through binding to its G-
573 protein coupled receptor, and this pathway is sufficient to trigger
574 neurodegeneration following infection [48]. Thus immune-inducible AMPs can have
575 striking interactions with neurological processes. Future studies characterizing the
576 role of *BaraA* in the erect wing phenotype should provide insight on interactions
577 between systemic immunity and host physiology.
578
579 Here we describe a complex immune effector gene that produces multiple
580 peptide products. *BaraA* encodes many of the most abundant immune effectors
581 induced downstream of the Toll signalling pathway, and indeed *BaraA* promotes
582 survival upon fungal infection. How each peptide contributes to the immune
583 response and/or erect wing behaviour will be informative in understanding the
584 range of effects immune effectors can have on host physiology. This work and others
585 also clarifies how the cocktail of immune effectors produced upon infection acts
586 specifically during innate host defence reactions.
587

588 **Materials and methods:**

589

590 *Fly genetics and sequence comparisons*

591

592 Sequence files were collected from FlyBase [49] and recently-generated
593 sequence data [44,50] and comparisons were made using Geneious R10. Putative
594 NF-κB binding sites were annotated using the Relish motif "GGRDNNHHBS"
595 described in Copley et al. [18] and a manually curated amalgam motif of
596 "GGGHHNNDVH" derived from common Dif binding sites described previously
597 [17,19]. Gene expression analyses were performed using primers described in
598 **Supplementary data file 1**, and further microarray validation for *BaraA* expression
599 comes from De Gregorio et al. [11].
600
601 The *UAS-BaraA* and *BaraA-Gal4* constructs were generated using the TOPO
602 pENTR entry vector and cloned into the pTW or pBPGUw Gateway™ vector systems
603 respectively. The *BaraA-Gal4* promoter contains 1675bp upstream of *BaraA1* (but
604 also *BaraA2,* sequence in supplementary information). The *BaraA-Gal4* construct
605 was inserted into the VK33 attP docking site (BDSC line #24871). The $BaraA^{SW1}$
606 (*ΔBaraA)* mutant was generated using CRISPR with two gRNAs and an HDR vector
607 by cloning 5' and 3' region-homologous arms into the pHD-dsRed vector, and
608 consequently *ΔBaraA* flies express dsRed in their eyes, ocelli, and abdomen. *ΔBaraA*
609 was generated in the Bloomington stock BL51323 as this background contains only
610 one copy of the *BaraA* locus. The induction of the immune response in these flies
611 was validated by qPCR and MALDI-TOF proteomics, wherein we discovered an
612 aberrant *Dso2* locus in the BL51323 background. We thus backcrossed the *ΔBaraA*
613 mutation once with a standard w^{1118} background and screened for wild-type *Dso2*
614 before use in any survival experiments. Additionally, *ΔBaraA* was isogenized into
615 the *DrosDel* w^{1118} isogenic background for seven generations before use in isogenic
616 fly experiments as described in Ferreira et al. [28].
617
618 A full description of fly stocks used for crosses and in experiments is provided in
619 **Supplementary data file 1**.
620
621 *Microbe culturing conditions*
622

623 Bacteria and *C. albicans* yeast were grown to mid-log phase shaking at
624 200rpm in their respective growth media (LB, BHI, or YPG) and temperature
625 conditions, and then pelleted by centrifugation to concentrate microbes. Resulting
626 cultures were diluted to the desired optical density at 600nm (OD) for survival
627 experiments as indicated. The following microbes were grown at 37°C: *Escherichia*
628 *coli strain 1106* (LB), *Enterococcus faecalis* (BHI), and *Candida albicans* (YPG). The
629 following microbes were grown at 29°C: *Erwinia carotovora carotovora (Ecc15)* (LB)
630 and *Micrococcus luteus* (LB). For filamentous fungi and molds, *Aspergillus fumigatus*
631 was grown at 37°C, and *Neurospora crassa* and *Beauveria bassiana* were grown at
632 room temperature on Malt Agar in the dark until sporulation. *Beauveria bassiana*
633 *strain R444* commercial spores were produced by Andermatt Biocontrol, product
634 BB-PROTEC.
635
636 *Survival experiments*
637
638 Survival experiments were performed as previously described [15], with 20
639 flies per vial with 2-3 replicate experiments. 3-5 day old males were used in
640 experiments unless otherwise specified. For fungi natural infections, flies were
641 flipped at the end of the first day to remove excess fungal spores from the vials.
642 Otherwise, flies were flipped thrice weekly. Statistical analyses were performed
643 using a Cox proportional hazards (CoxPH) model in R 3.6.3. We report the hazard
644 ratio (HR) alongside p-values as a proxy for effect size in survival experiments.
645 Throughout our analyses, we required $p < .05$ as evidence to report an effect as
646 significant, but note interactions with $|HR| > 0.5$ as potentially important provided α
647 approached .05, and tamp down importance of interactions that were significant,
648 but have relatively minor effect size ($|HR| < 0.5$).
649
650 *Erect wing scoring*
651

652 The erect wing phenotype was scored as the number of flies with splayed
653 wings throughout a distinct majority of the period of observation (30s); if unclear,
654 the vial was monitored an additional 30s. Here we define splayed wings as wings
655 not at rest over the back, but did not require wings to be fully upright; on occasion
656 wings were held splayed outward at ~45° relative to the dorsal view, and often
657 slightly elevated relative to the resting state akin to male aggressive displays.
658 Sometimes only one wing was extended, which occurred in both thoracic pricking
659 and fungi natural infections; these flies were counted as having erect wing. In
660 natural infections, the typical course of erect wing display developed in two fashions
661 at early time points, either: i) flies beginning with wings slightly splayed but not
662 fully upright, or ii) flies constantly flitting their wings outward and returning them
663 to rest briefly, only to flit them outward again for extended periods of time. Shortly
664 after infection, some flies were also observed wandering around with wings beating
665 at a furious pace, which was not counted as erect wing. However at later time points
666 erect wing flies settled more permanently on upright splayed wings. Erect wing
667 measurements were taken daily following infection, and erect wing flies over total
668 flies was converted to a percent. Data points in **Fig.** 5B-D represent % with erect
669 wing in individual replicate experiments with ~20 flies per vial. Flies stuck in the
670 vial, or where the wings had become sticky or mangled were not included in totals.
671 **Table S1** reports mean percentages across replicate experiments for all pathogens
672 and genotypes where erect wing was monitored. Days post-infection reported in
673 **Table S1** were selected as the final day prior to major incidents of mortality. For *E.*
674 *faecalis* live infections, $Bom^{\Delta 55C}$ and spz^{rm7} erect wing was taken at 1dpi due to major
675 mortality events by 2dpi specifically in these lines.
676
677 Erect wing measurements were performed in parallel with survival
678 experiments, which often introduced injury to the thorax below the wing possibly
679 damaging flight muscle. It is unlikely that muscle damage explains differences in
680 erect wing display. First: we noticed erect wing initially during natural infections
681 with *A. fumigatus*, and observed erect wing upon *B. bassiana R444* and *Metarhizium*

682 *rileyi PHP1705* natural infections (**Table S1**; *M. rileyi* = NOMU-PROTEC, Andermatt
683 Biocontrol). Second: only 1 of 75 total *iso* w^{1118} males displayed erect wing across 4
684 systemic infection experiments with *E. faecalis*. For comparison: 19 of 80 total *iso*
685 *ΔBaraA* and 48 of 80 *w; ΔBaraA* flies displayed erect wing (**Table S1**). Future studies
686 might be better served using an abdominal infection mode, which can have different
687 infection dynamics [51]. However we find erect wing display to be robust upon
688 either septic injury or natural infection modes.
689
690 *IM10-like peptide in vitro activity*
691
692 The 23-residue Baramicin peptides were synthesized by GenicBio to a purity
693 of >95%, verified by HPLC. An N-terminal pyroglutamate modification was included
694 based on previous peptidomic descriptions of Baramicins IM10, IM12, and IM13
695 [52], which we also detected in our LC-MS data (**Fig.** S2). Peptides were dissolved in
696 DMSO and diluted to a working stock of 1200μM in 0.6% DMSO; the final
697 concentration for incubations was 300μM in 0.15% DMSO. For microbe-killing
698 assays, microbes were allowed to grow to log-growth phase, at which point they
699 were diluted to ~50cells/μL. Two μL of culture (~100 cells), and 1μL water or
700 antibiotic was mixed with 1μL of a 1:1:1 cocktail of IM10, IM12, and IM13 peptides
701 to a final concentration of 300μM total peptides; 1μL of water + DMSO (final
702 concentration = 0.15% DMSO) was used as a negative control. Four μL microbe-
703 peptide solutions were incubated for 24h at 4°C. Microbe-peptide cultures were
704 then diluted to a final volume of 100μL and the entire solution was plated on LB
705 agar or BiGGY agar plates. Colonies were counted manually. For combinatorial
706 assays with bacteria, *C. albicans* yeast, and *B. bassiana R444* spores, peptide cocktails
707 were combined with membrane disrupting antimicrobials effective against relevant
708 pathogens beginning at: 10 μM Cecropin A (Sigma), 500μg/mL ampicillin, or
709 250μg/mL Pimaricin (commercially available as "Fungin," InVivogen), serially
710 diluted through to 0.1 μM, 0.5μg/mL, and 4μg/mL respectively.
711

712 *Beauveria bassiana R444* spores were prepared by dissolving ~30mg of
713 spores in 10mL PBS, and then 4μL microbe-peptide solutions were prepared as
714 described for *C. albicans* followed by incubation for 24h at 4°C; this spore density
715 was optimal in our hands to produce distinct individual colonies. Then, 4μL PBS was
716 added to each solution and 2μL droplets were plated on malt agar at 25°C. Colony
717 diameters were measured 4 days after plating by manually analyzing images.
718 Experimental replicates were included as co-variates in One-way ANOVA analysis.
719 The initial dataset approached violating Shapiro-Wilk assumptions of normality (p =
720 0.061) implemented in R 3.6.3. We subsequently removed four colonies from the
721 analysis, as these outliers were over two standard deviations lower than their
722 respective mean (removed colonies: PBS 0.15cm, PBS 0.25cm, IM10-like+Pimaricin
723 0.21cm, and a second IM10-like+Pimaricin colony of 0.21cm); the resulting Shapiro-
724 Wilk p-value = 0.294, and both QQ and residual plots suggested a normal
725 distribution. Final killing activities and colony diameters were compared by One-
726 way ANOVA with Holm-Sidak multiple test correction (*C. albicans*) and Tukey's
727 honest significant difference multiple test correction (*B. bassiana R444*).
728
729 *Gene expression analyses*
730
731 RNA was extracted using TRIzol according to manufacturer's protocol. cDNA
732 was reverse transcribed using Takara Reverse Transcriptase. qPCR was performed
733 using PowerUP mastermix from Applied Biosystems at 60°C using primers listed in
734 **Supplementary data file 1**. Gene expression was quantified using the PFAFFL
735 method [53] with *Rp49* as the reference gene. Statistical analysis was performed by
736 One-way ANOVA with Holm-Sidak's multiple test correction or student's t-test.
737 Error bars represent one standard deviation from the mean.
738
739 *Proteomic analyses*
740

741 Raw haemolymph samples were collected from immune-challenged flies for
742 MALDI-TOF proteomic analysis as described in [14,15]. MALDI-TOF proteomic
743 signals were confirmed independently at facilities in both San Diego, USA and
744 Lausanne, CH. In brief, haemolymph was collected by capillary and transferred to
745 0.1% TFA before addition to acetonitrile universal matrix. Representative spectra
746 are shown. Peaks were identified via corresponding m/z values from previous
747 studies [8,21]. Spectra were visualized using mMass, and figures were additionally
748 prepared using Inkscape v0.92.
749
750 **Author contributions:**
751
752 MAH planned experiments, performed bioinformatic analyses, infection
753 experiments, and in vitro assays. BL supervised the project and MAH and BL wrote
754 the manuscript. LC planned and generated the *BaraA* deletion and performed key
755 descriptive experiments and observations. AM assisted with infection and in vitro
756 assays. II, and SAW generated and supplied critical reagents and provided
757 constructive commentary.
758
759 **Acknowledgements:**
760
761 This research was supported by Sinergia grant CRSII5_186397 and Novartis
762 Foundation 532114 awarded to Bruno Lemaitre, and by National Institute of Health
763 (NIH) grant R01 GM050545 to Steven Wasserman. We thank Jean-Philippe Boquete
764 for assistance with the generation of Gal4 and UAS constructs. We would also like to
765 acknowledge the technical expertise provided by the proteomics and mass
766 spectrometry facilities in both UCSD and EPFL, and specifically We further thank
767 Huang et al. (*in preparation*) for their cooperation in publishing initial descriptions
768 of the *BaraA* gene, and for stimulating discussion.
769
770

773 **References:**

774

775 1. Lemaitre B, Hoffmann J. The Host Defense of Drosophila Melanogaster. Annual
776 Review of Immunology. 2007;25: 697–743.
777 doi:10.1146/annurev.immunol.25.022106.141615

778 2. Kurz CL, Ewbank JJ. Caenorhabditis elegans: An emerging genetic model for the
779 study of innate immunity. Nature Reviews Genetics. 2003;4: 380–390.
780 doi:10.1038/nrg1067

781 3. Kaufmann SHE. Immunology's foundation: the 100-year anniversary of the
782 Nobel Prize to Paul Ehrlich and Elie Metchnikoff. Nat Immunol. 2008;9: 705–
783 712. doi:10.1038/ni0708-705

784 4. Steiner H, Hultmark D, Engström \AA, Bennich H, Boman HG. Sequence and
785 specificity of two antibacterial proteins involved in insect immunity. Nature.
786 1981;292: 246–248. doi:10.1038/292246a0

787 5. Lemaitre B, Nicolas E, Michaut L, Reichhart JM, Hoffmann JA. The dorsoventral
788 regulatory gene cassette spatzle/Toll/Cactus controls the potent antifungal
789 response in Drosophila adults. Cell. 1996;86: 973–983. doi:10.1016/S0092-
790 8674(00)80172-5

791 6. Lemaitre B, Reichhart JM, Hoffmann JA. Drosophila host defense: differential
792 induction of antimicrobial peptide genes after infection by various classes of
793 microorganisms. Proceedings of the National Academy of Sciences of the United
794 States of America. 1997;94: 14614–9. doi:10.1073/pnas.94.26.14614

795 7. Lemaitre B, Kromer-Metzger E, Michaut L, Nicolas E, Meister M, Georgel P, et al.
796 A recessive mutation, immune deficiency (imd), defines two distinct control
797 pathways in the Drosophila host defense. Proc Natl Acad Sci U S A. 1995;92:
798 9465–9469. doi:10.1073/pnas.92.21.9465

799 8. Uttenweiler-Joseph S, Moniatte M, Lagueux M, Van Dorsselaer a, Hoffmann J a,
800 Bulet P. Differential display of peptides induced during the immune response of
801 Drosophila: a matrix-assisted laser desorption ionization time-of-flight mass
802 spectrometry study. Proceedings of the National Academy of Sciences of the
803 United States of America. 1998;95: 11342–11347.
804 doi:10.1073/pnas.95.19.11342

805 9. Lazzaro BP, Zasloff M, Rolff J. Antimicrobial peptides: Application informed by
806 evolution. Science. 2020;368. doi:10.1126/science.aau5480

807 10. Hanson MA, Lemaitre B. New insights on Drosophila antimicrobial peptide
808 function in host defense and beyond. Curr Opin Immunol. 2020;62: 22–30.
809 doi:10.1016/j.coi.2019.11.008

810 11. De Gregorio E, Spellman PT, Tzou P, Rubin GM, Lemaitre B. The Toll and Imd
811 pathways are the major regulators of the immune response in Drosophila.
812 EMBO Journal. 2002;21: 2568–2579. doi:10.1093/emboj/21.11.2568

813 12. Clemmons AW, Lindsay SA, Wasserman SA. An Effector Peptide Family
814 Required for Drosophila Toll-Mediated Immunity. PLoS Pathogens. 2015;11.
815 doi:10.1371/journal.ppat.1004876

816 13. Lindsay SA, Lin SJH, Wasserman SA. Short-Form Bomanins Mediate Humoral
817 Immunity in Drosophila. 2018. doi:10.1159/000489831

818 14. Cohen LB, Lindsay SA, Xu Y, Lin SJH, Wasserman SA. The Daisho Peptides
819 Mediate Drosophila Defense Against a Subset of Filamentous Fungi. Front
820 Immunol. 2020;11: 9. doi:10.3389/fimmu.2020.00009

821 15. Hanson MA, Dostálová A, Ceroni C, Poidevin M, Kondo S, Lemaitre B. Synergy
822 and remarkable specificity of antimicrobial peptides in vivo using a systematic
823 knockout approach. eLife. 2019;8. doi:10.7554/elife.44341

824 16. Unckless RL, Howick VM, Lazzaro BP. Convergent Balancing Selection on an
825 Antimicrobial Peptide in Drosophila. Current Biology. 2016;26: 257–262.
826 doi:10.1016/j.cub.2015.11.063

827 17. Busse MS, Arnold CP, Towb P, Katrivesis J, Wasserman SA. A κB sequence code
828 for pathway-specific innate immune responses. EMBO Journal. 2007;26: 3826–
829 3835. doi:10.1038/sj.emboj.7601798

830 18. Copley RR, Totrov M, Linnell J, Field S, Ragoussis J, Udalova IA. Functional
831 conservation of Rel binding sites in drosophilid genomes. Genome Research.
832 2007;17: 1327–1335. doi:10.1101/gr.6490707

833 19. Tanji T, Yun E-Y, Ip YT. Heterodimers of NF-κB transcription factors DIF and
834 Relish regulate antimicrobial peptide genes in Drosophila. Proceedings of the
835 National Academy of Sciences. 2010;107: 14715–14720.
836 doi:10.1073/pnas.1009473107

837 20. Ferrandon D, Jung AC, Criqui MC, Lemaitre B, Uttenweiler-Joseph S, Michaut L,
838 et al. A drosomycin-GFP reporter transgene reveals a local immune response in
839 Drosophila that is not dependent on the Toll pathway. EMBO Journal. 1998;17:
840 1217–1227. doi:10.1093/emboj/17.5.1217

841 21. Levy F, Rabel D, Charlet M, Bulet P, Hoffmann JA, Ehret-Sabatier L. Peptidomic
842 and proteomic analyses of the systemic immune response of Drosophila.
843 Biochimie. 2004;86: 607–616. doi:10.1016/j.biochi.2004.07.007

844 22. Tzou P, Reichhart J-M, Lemaitre B. Constitutive expression of a single
845 antimicrobial peptide can restore wild-type resistance to infection in
846 immunodeficient Drosophila mutants. Proceedings of the National Academy of
847 Sciences of the United States of America. 2002;99: 2152–2157.
848 doi:10.1073/pnas.042411999

849 23. Wiegand I, Hilpert K, Hancock REW. Agar and broth dilution methods to
850 determine the minimal inhibitory concentration (MIC) of antimicrobial
851 substances. Nature Protocols. 2008. doi:10.1038/nprot.2007.521

852 24. Rabel D, Charlet M, Ehret-Sabatier L, Cavicchioli L, Cudic M, Otvos L, et al.
853 Primary Structure and in Vitro Antibacterial Properties of the Drosophila
854 melanogaster Attacin C Pro-domain. Journal of Biological Chemistry. 2004;279:
855 14853–14859. doi:10.1074/jbc.M313608200

856 25. Rahnamaeian M, Cytry ska M, Zdybicka-Barabas A, Dobslaff K, Wiesner J,
857 Twyman RM, et al. Insect antimicrobial peptides show potentiating functional
858 interactions against Gram-negative bacteria. Proceedings of the Royal Society
859 B: Biological Sciences. 2015;282: 20150293–20150293.
860 doi:10.1098/rspb.2015.0293

861 26. Kragol G, Lovas S, Varadi G, Condie BA, Hoffmann R, Otvos L. The antibacterial
862 peptide pyrrhocoricin inhibits the ATPase actions of DnaK and prevents
863 chaperone-assisted protein folding. Biochemistry. 2001;40: 3016–3026.
864 doi:10.1021/bi002656a

865 27. Ryder E, Blows F, Ashburner M, Bautista-Llacer R, Coulson D, Drummond J, et
866 al. The DrosDel collection: A set of P-element insertions for generating custom
867 chromosomal aberrations in Drosophila melanogaster. Genetics. 2004;167:
868 797–813. doi:10.1534/genetics.104.026658

869 28. Ferreira ÁG, Naylor H, Esteves SS, Pais IS, Martins NE, Teixeira L. The Toll-
870 dorsal pathway is required for resistance to viral oral infection in Drosophila.
871 PLoS Pathog. 2014;10: e1004507. doi:10.1371/journal.ppat.1004507

872 29. Levashina EA, Ohresser S, Bulet P, Reichhart J -M, Hetru C, Hoffmann JA.
873 Metchnikowin, a Novel Immune-Inducible Proline-Rich Peptide from
874 Drosophila with Antibacterial and Antifungal Properties. European Journal of
875 Biochemistry. 1995;233: 694–700. doi:10.1111/j.1432-1033.1995.694_2.x

876 30. Fehlbaum P, Bulet P, Michaut L, Lagueux M, Broekaert WF, Hetru C, et al. Insect
877 immunity: Septic injury of drosophila induces the synthesis of a potent

878 antifungal peptide with sequence homology to plant antifungal peptides.
879 Journal of Biological Chemistry. 1994;269: 33159–33163.

880 31. Dudzic JP, Hanson MA, Iatsenko I, Kondo S, Lemaitre B. More Than Black or
881 White: Melanization and Toll Share Regulatory Serine Proteases in Drosophila.
882 Cell Reports. 2019;27: 1050–1061.e3. doi:10.1016/j.celrep.2019.03.101

883 32. Binggeli O, Neyen C, Poidevin M, Lemaitre B. Prophenoloxidase Activation Is
884 Required for Survival to Microbial Infections in Drosophila. PLoS Pathogens.
885 2014;10. doi:10.1371/journal.ppat.1004067

886 33. DeSimone SM, White K. The Drosophila erect wing gene, which is important for
887 both neuronal and muscle development, encodes a protein which is similar to
888 the sea urchin P3A2 DNA binding protein. Mol Cell Biol. 1993;13: 3641–3649.
889 doi:10.1128/MCB.13.6.3641

890 34. Elya C, Lok TC, Spencer QE, McCausland H, Martinez CC, Eisen M. Robust
891 manipulation of the behavior of Drosophila melanogaster by a fungal pathogen
892 in the laboratory. eLife. 2018;7: e34414. doi:10.7554/eLife.34414

893 35. Imler J-L, Bulet P. Antimicrobial peptides in Drosophila: structures, activities
894 and gene regulation. Chemical immunology and allergy. 2005;86: 1–21.
895 doi:10.1159/000086648

896 36. Hedengren M, Borge K, Hultmark D. Expression and evolution of the Drosophila
897 attacin/diptericin gene family. Biochemical and biophysical research
898 communications. 2000;279: 574–81. doi:10.1006/bbrc.2000.3988

899 37. Khush RS, Lemaitre B. Genes that fight infection: what the Drosophila genome
900 says about animal immunity. Trends Genet. 2000;16: 442–449.
901 doi:10.1016/s0168-9525(00)02095-3

902 38. Goto A, Yano T, Terashima J, Iwashita S, Oshima Y, Kurata S. Cooperative
903 regulation of the induction of the novel antibacterial Listericin by
904 peptidoglycan recognition protein LE and the JAK-STAT pathway. J Biol Chem.
905 2010;285: 15731–15738. doi:10.1074/jbc.M109.082115

906 39. Barajas-azpeleta R, Wu J, Gill J, Welte R. Antimicrobial peptides modulate long-
907 term memory. PLoS Genetics. 2018; 1–26. doi:10.1371/journal.pgen.1007440

908 40. Steffen H, Rieg S, Wiedemann I, Kalbacher H, Deeg M, Sahl H-G, et al. Naturally
909 processed dermicidin-derived peptides do not permeabilize bacterial
910 membranes and kill microorganisms irrespective of their charge. Antimicrob
911 Agents Chemother. 2006;50: 2608–2620. doi:10.1128/AAC.00181-06

912 41. Zdybicka-Barabas A, Mak P, Klys A, Skrzypiec K, Mendyk E, Fiołka MJ, et al.
913 Synergistic action of Galleria mellonella anionic peptide 2 and lysozyme against

914 Gram-negative bacteria. Biochim Biophys Acta. 2012;1818: 2623–2635.
915 doi:10.1016/j.bbamem.2012.06.008

916 42. Hanson MA, Lemaitre B, Unckless RL. Dynamic Evolution of Antimicrobial
917 Peptides Underscores Trade-Offs Between Immunity and Ecological Fitness.
918 Frontiers in Immunology. 2019;10: 2620. doi:doi: 10.3389/fimmu.2019.02620

919 43. Casteels-Josson K, Capaci T, Casteels P, Tempst P. Apidaecin multipeptide
920 precursor structure: a putative mechanism for amplification of the insect
921 antibacterial response. The EMBO journal. 1993;12: 1569–78.
922 doi:10.1002/j.1460-2075.1993.tb05801.x

923 44. Hanson MA, Hamilton PT, Perlman SJ. Immune genes and divergent
924 antimicrobial peptides in flies of the subgenus Drosophila. BMC evolutionary
925 biology. 2016;16: 228. doi:10.1186/s12862-016-0805-y

926 45. Brogden KA, Guthmiller JM, Salzet M, Zasloff M. The nervous system and innate
927 immunity: The neuropeptide connection. Nature Immunology. 2005. pp. 558–
928 564. doi:10.1038/ni1209

929 46. Koganezawa M, Haba D, Matsuo T, Yamamoto D. The Shaping of Male Courtship
930 Posture by Lateralized Gustatory Inputs to Male-Specific Interneurons. Current
931 Biology. 2010;20: 1–8. doi:10.1016/j.cub.2009.11.038

932 47. Kurz CL, Charroux B, Chaduli D, Viallat-Lieutaud A, Royet J. Peptidoglycan
933 sensing by octopaminergic neurons modulates Drosophila oviposition. Elife.
934 2017;6. doi:10.7554/eLife.21937

935 48. Lezi E, Zhou T, Koh S, Chuang M, Sharma R, Pujol N, et al. An Antimicrobial
936 Peptide and Its Neuronal Receptor Regulate Dendrite Degeneration in Aging
937 and Infection. Neuron. 2018;97: 125-138.e5. doi:10.1016/j.neuron.2017.12.001

938 49. Gramates LS, Marygold SJ, Dos Santos G, Urbano JM, Antonazzo G, Matthews BB,
939 et al. FlyBase at 25: Looking to the future. Nucleic Acids Research. 2017;45:
940 D663–D671. doi:10.1093/nar/gkw1016

941 50. Hill T, Koseva BS, Unckless RL. The genome of Drosophila innubila reveals
942 lineage-specific patterns of selection in immune genes. Molecular Biology and
943 Evolution. 2019. doi:10.1093/molbev/msz059

944 51. Chambers MC, Jacobson E, Khalil S, Lazzaro BP. Thorax injury lowers resistance
945 to infection in Drosophila melanogaster. Infect Immun. 2014;82: 4380–4389.
946 doi:10.1128/IAI.02415-14

947 52. Verleyen P, Baggerman G, D'Hertog W, Vierstraete E, Husson SJ, Schoofs L.
948 Identification of new immune induced molecules in the haemolymph of

949 Drosophila melanogaster by 2D-nanoLC MS/MS. Journal of Insect Physiology.
950 2006;52: 379–388. doi:10.1016/j.jinsphys.2005.12.007

951 53. Pfaffl MW. A new mathematical model for relative quantification in real-time
952 RT-PCR. Nucleic Acids Res. 2001;29: e45. doi:10.1093/nar/29.9.e45

953 54. Tyler-Cross R, Schirch V. Effects of amino acid sequence, buffers, and ionic
954 strength on the rate and mechanism of deamidation of asparagine residues in
955 small peptides. J Biol Chem. 1991;266: 22549–22556.

956

Supplemental figure captions:

Figure S1: A-F) AMP and *BaraA* expression dynamics upon injury with a mixture of *E. coli* and *M. luteus* (A,D,E,F) and natural infection with *B. bassiana* (B,C), from De Gregorio et al. (2002). **A)** *BaraA* immediate expression dynamics are more similar to *Drs* (Toll and some Imd) than *BomBc3* (Toll-specific). **B)** Natural infection by *B. bassiana* results in sustained *BaraA* expression for days. **C)** Fungus-induced *BaraA* expression is abolished in spz^{rm7} mutants. **D-E)** *BaraA* is induced by bacteria in Rel^{E20} mutants **(D)**, but far less in spz^{rm7} mutants **(E)**. **F)** *BaraA* induction is completely abolished in *Rel, spz* double mutants. **G)** 400bp of upstream sequence from *BaraA* annotated with putative *Rel* or *Dif/dl* binding sites (included in supplemental data file 1). **H)** Expression of *BaraA in wild-type* and spz^{rm7} *flies* following injury with the Gram-positive bacteria *M. luteus* . **I)** The *BaraA>mGFP* reporter line shows more robust induction of GFP 60hpi by pricking with *M. luteus* than *E. coli*. **J)** Expression of *BaraA>mGFP* in the spermatheca of females (yellow arrow). Representative images shown.

Figure S2: LCMS coverage of trypsin-digested and detected BaraA peptides aligned to the protein coding sequence. Peptide fragments cover the whole precursor protein barring furin site-associated motifs. Additionally, two peptide fragments are absent: i) the first 4 residues of the C-terminus ("GIND," not predicted *a priori*), and ii) the C-terminus peptide's "RPDGR" motif, which is predicted as a degradation product of Trypsin cleavage and whose size is beyond the minimum range of detection. Without the GIND motif, the mass of the contiguous C-terminus is 5974.5 Da, matching the mass observed by MALDI-TOF for IM22 (**Fig.** 2A). The N-terminal Q residues of IM10, IM12, IM13, and IM24 are pyroglutamate-modified, as described previously [2]. The asparagine residues of IM10-like peptides are sometimes deamidated, likely as a consequence of our 0.1% TFA sample collection method as "NG" motifs are deamidated in acidic conditions [54].

Figure S3: A) Aligned IM22 peptides of *Drosophila Baramicin A-like* genes, with the IM10-like 'VWKRPDGRTV' motif noted. The GIND residues at the N-terminus are cleaved off in *Dmel\BaraA*, and this site is similarly cleaved at RXRR furin cleavage site in subgenus Drosophila flies. **B)** Alignment of the three IM10-like peptides of *D. melanogaster BaraA* with the "VXRPXRTV" motif noted.

Figure S4: *Over-expression of BaraA partially* rescues *Rel, spz* double mutant susceptibility to infection in both males and females. A) Overexpressing *BaraA* modestly improves survival of *Rel, spz* flies upon injury with *Ecc15*, though initial mortality closely resembles that of *Rel, spz* controls, and the differences observed in males were not significant (p = .106). **B)** Overexpressing *BaraA* did not improve the survival of *Rel, spz* flies upon *E. coli* infection. **C)** Overexpressing *BaraA* only marginally improves survival of *Rel, spz* females, but not males, upon *M. luteus* infections. Infections using a higher dose tended to kill 100% of *Rel, spz* flies regardless of sex or expression of *BaraA*, suggesting that if *BaraA* overexpression

does affect susceptibility to *M. luteus*, this effect is possible within only a narrow window of *M. luteus* concentration. **D-F)** Overexpressing *BaraA* improves survival of *Rel, spz* male and female flies upon injury with *C. albicans* **(D)** or natural infection with *A. fumigatus* **(E)** and *N. crassa* **(F).** P-values are shown for each biological sex in an independent CoxPH model not including the other sex relative to *Rel, spz* as a reference.

Figure S5: RT-qPCR shows that the expression of *BomBc3* **(A)** *Drs* **(B)** and *DptA* **(C)** in wild-type 18hpi in *iso ΔBaraA* flies.

Figure S6: Additional survivals using *ΔBaraA* flies in two distinct genetic backgrounds upon infection by a diversity of microbes. A) No significant susceptibility of *ΔBaraA* flies to *Ecc15* infection. **B)** *iso ΔBaraA* but not *w; ΔBaraA* flies are susceptible to *P. burhodogranariea*, **C)** *w; ΔBaraA but not iso ΔBaraA* flies exhibit a minor susceptibility to *B. subtilis* (HR > 0.5, p = .099). **D)** Both *w; ΔBaraA* and *iso ΔBaraA* exhibit a minor increased susceptibility to *C. albicans*, though the ultimate survival rate was not significantly different from their respective wild-types. Dotted line indicates CoxPH statistical signature when censored at 2dpi. **E-F)** *w; ΔBaraA* males are slightly susceptible to *A. fumigatus* natural infection (HR > 0.5, p = .078), but not females, nor isogenic flies. Additional infections using *ΔBaraA,* $Bom^{\Delta 55C}$ double mutant flies reveal that *BaraA* mutation increases the susceptibility of $Bom^{\Delta 55C}$ flies in both males and females (cumulative curves shown in **Fig.** 4C). Blue backgrounds = Gram-negative bacteria, orange backgrounds = Gram-positive bacteria, yellow backgrounds = fungi.

Figure S7: Additional survival analyses reveal only a minor contribution of *BaraA* to defence against infection by *E. faecalis*. A) Crossing with a genomic deficiency (*Df(BaraA)*) leads to increased susceptibility in both the *w* background and isogenic DrosDel background, with *Df(BaraA)/ΔBaraA* flies suffering the greatest mortality in either crossing scheme. Both deficiency crosses yielded an earlier susceptibility in *BaraA*-deficient flies (shown with dotted black lines), however neither experiment ultimately reached statistical significance. **B)** *BaraA* RNAi flies (*Act>BaraA-IR*) suffered greater mortality than *Act>OR-R* or *OR-R/BaraA-IR* controls, but this was not statistically significant at α = .05.

Figure S8: Additional survival analyses reveal a consistent contribution of *BaraA* to defence against natural infection with *B. bassiana*. A) Crossing with a genomic deficiency (*Df(BaraA)*) leads to increased susceptibility of *Df(BaraA)/ΔBaraA* flies for both the *w* background and isogenic DrosDel background relative to wild-type controls (p < .05). **B)** *Act>BaraA-IR* flies were more susceptible than *OR>BaraA-IR* (p = .004), although not significantly different from our *Act>OR-R* control (p = .266). **C)** Overexpressing *BaraA* (*Act>UAS-BaraA*) improved survival against *B. bassiana* relative to *Act>OR-R* controls (HR = -0.52, p = 0.010).

Figure S9: Frequency of erect wing display following additional challenges. A-B) Erect wing frequencies 2dpi after clean injury **(A)**, or *Ecc15* septic injury **(B)**. The erect wing frequencies of flies pricked by HK-*E. faecalis* (**Fig.** 6D) are overlaid in the background to facilitate direct comparison with the frequency observed upon Toll pathway activation. **C)** The frequency of erect wing display is increased following *E. faecalis* septic injury in *ΔBaraA/+* or *Df(BaraA)/+* flies. Data points are pooled from *w; ΔBaraA* and *iso ΔBaraA* crosses after *E. faecalis* infections shown in **Fig.** S7A and data in **Table** S1.

Table S1: Erect wing frequencies from various infection experiments. Following initial erect wing observations upon *A. fumigatus* natural infection, we scored erect wing frequency in all subsequent survival experiments. Data represent the mean % of males displaying erect wing ± one standard deviation. n exp = number of replicate experiments performed, and dpi ewg taken = days post-infection where erect wing data were recorded. We additionally performed natural infections with *Metarhizium rileyi* that generally did not cause significant mortality in flies, but nevertheless induced erect wing specifically in *ΔBaraA* males and spz^{rm7} controls. Bacterial infections were performed by septic injury, while fungal challenges were natural infections performed by rolling flies in spores.

Legend (A-F): BomBc3 Drs DptA BaraA

Figure S1

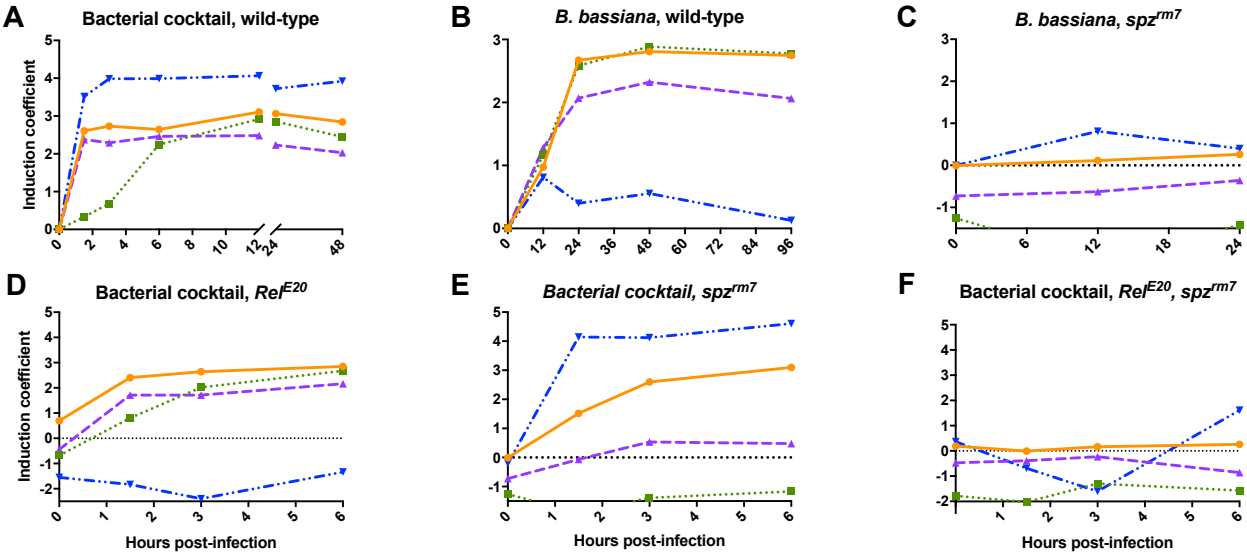

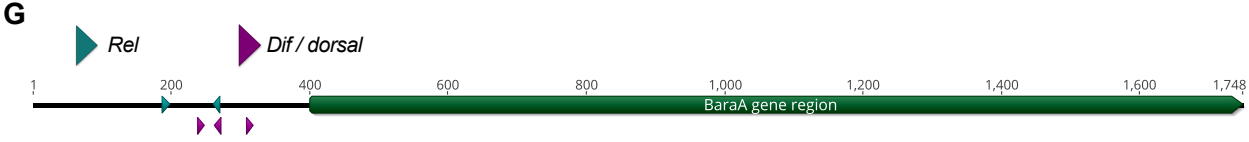

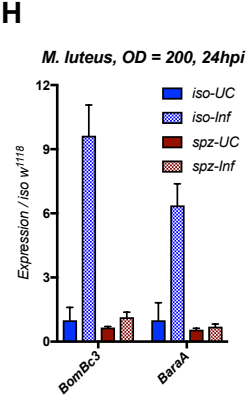

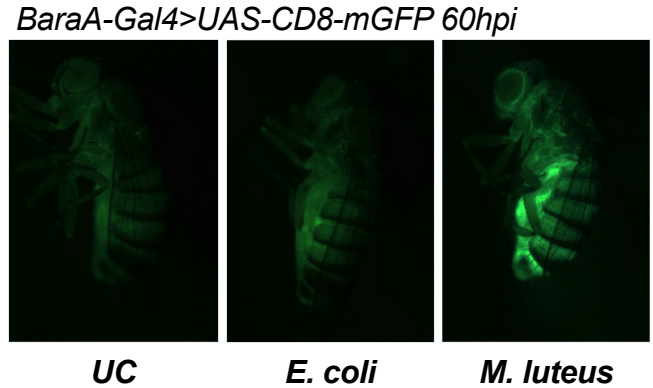

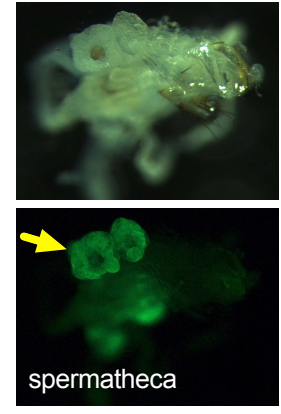

Figure S2

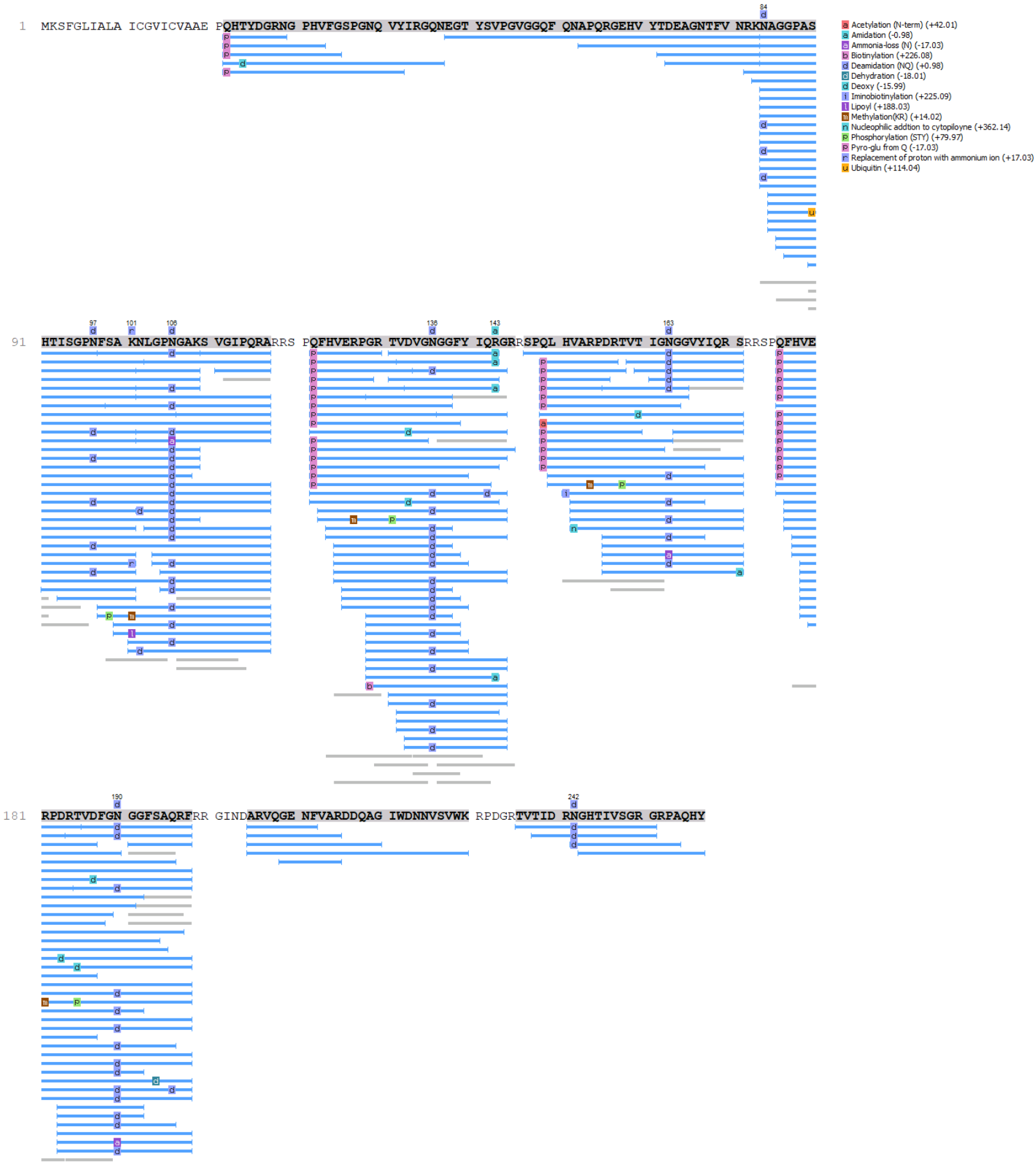
1 MKSFGLIALA ICGVICVAAE PQHTYDGRNG PHVFGSPGNQ VYIRGQNEGT YSVPGVGGQF QNAPQRGEHV YTDEAGNTFV NRKNAGGPAS
91 HTISGPNFSA KNLGPNGAKS VGIPQRARRS PQFHVERPGR TVDVGNGGFY IQRGRRSPQL HVARPDRTVT IGNGGVYIQR SRRSPQFHVE
181 RPDRTVDFGN GGFSAQRFRR GINDARVQGE NFVARDDQAG IWDNNVSVWK RPDGRTVTID RNGHTIVSGR GRPAQHY
a Acetylation (N-term) (+42.01)
a Amidation (-0.98)
a Ammonia-loss (N) (-17.03)
b Biotinylation (+226.08)
d Deamidation (NQ) (+0.98)
d Dehydration (-18.01)
d Deoxy (-15.99)
i Iminobiotinylation (+225.09)
l Lipoyl (+188.03)
m Methylation(KR) (+14.02)
n Nucleophilic addtion to cytopiloyne (+362.14)
p Phosphorylation (STY) (+79.97)
p Pyro-glu from Q (-17.03)
r Replacement of proton with ammonium ion (+17.03)
u Ubiquitin (+114.04)

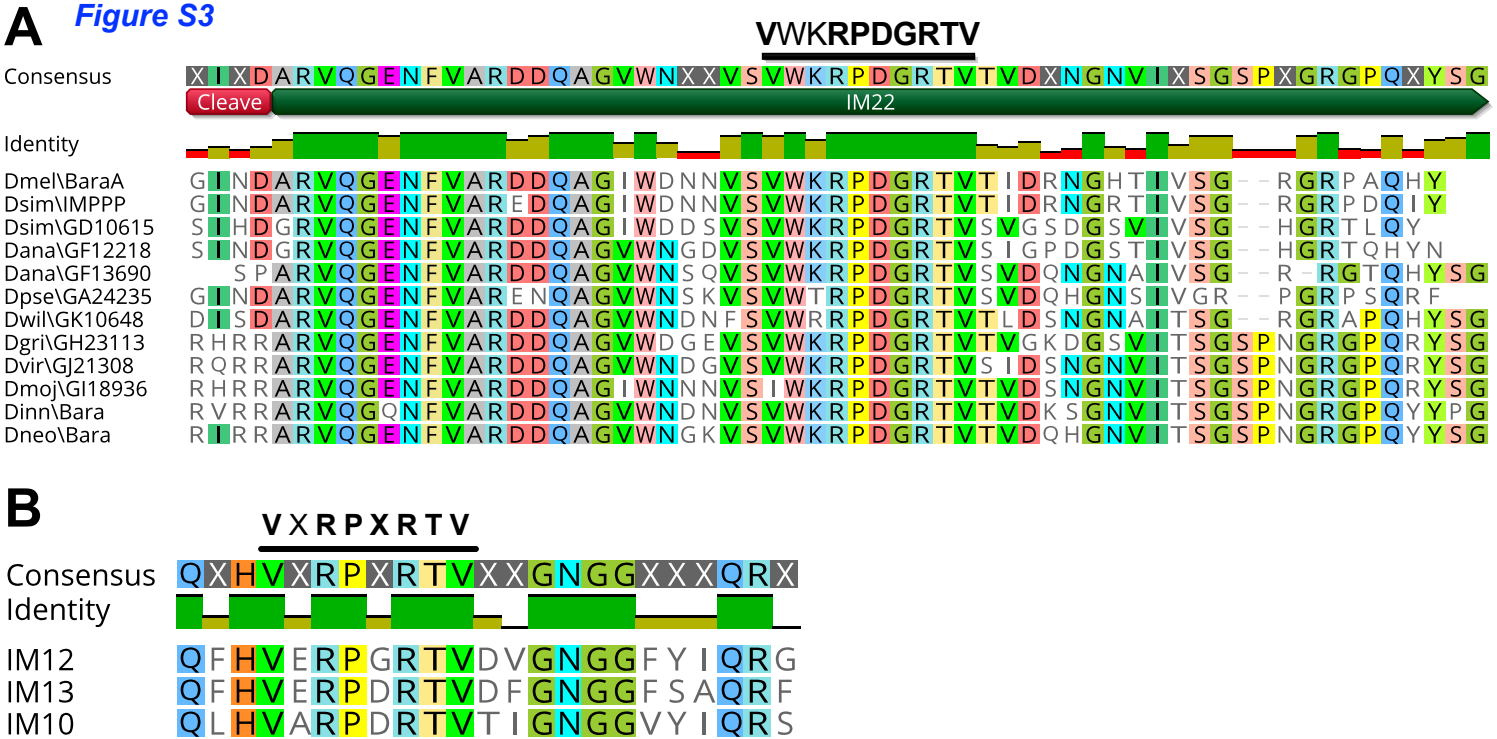
A
Figure S3
VWKRPDGRTV
Consensus
Cleave
IM22
Identity
Dmel\BaraA
Dsim\IMPPP
Dsim\GD10615
Dana\GF12218
Dana\GF13690
Dpse\GA24235
Dwil\GK10648
Dgri\GH23113
Dvir\GJ21308
Dmoj\GI18936
Dinn\Bara
Dneo\Bara
B
VXRPXRTV
Consensus
Identity
IM12
IM13
IM10

Legend A-F: +; Rel, spz — Act>BaraA; Rel, spz — OR-R

Figure S4

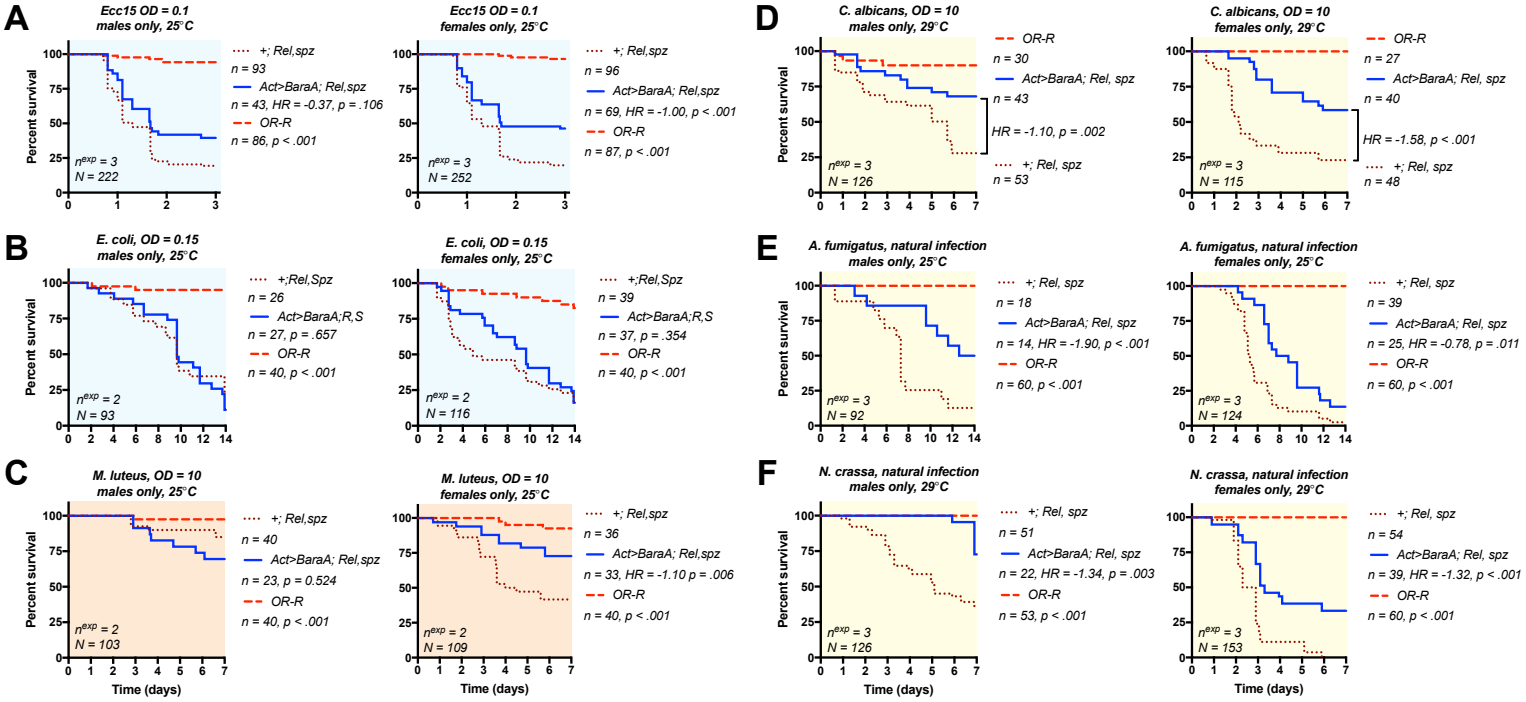

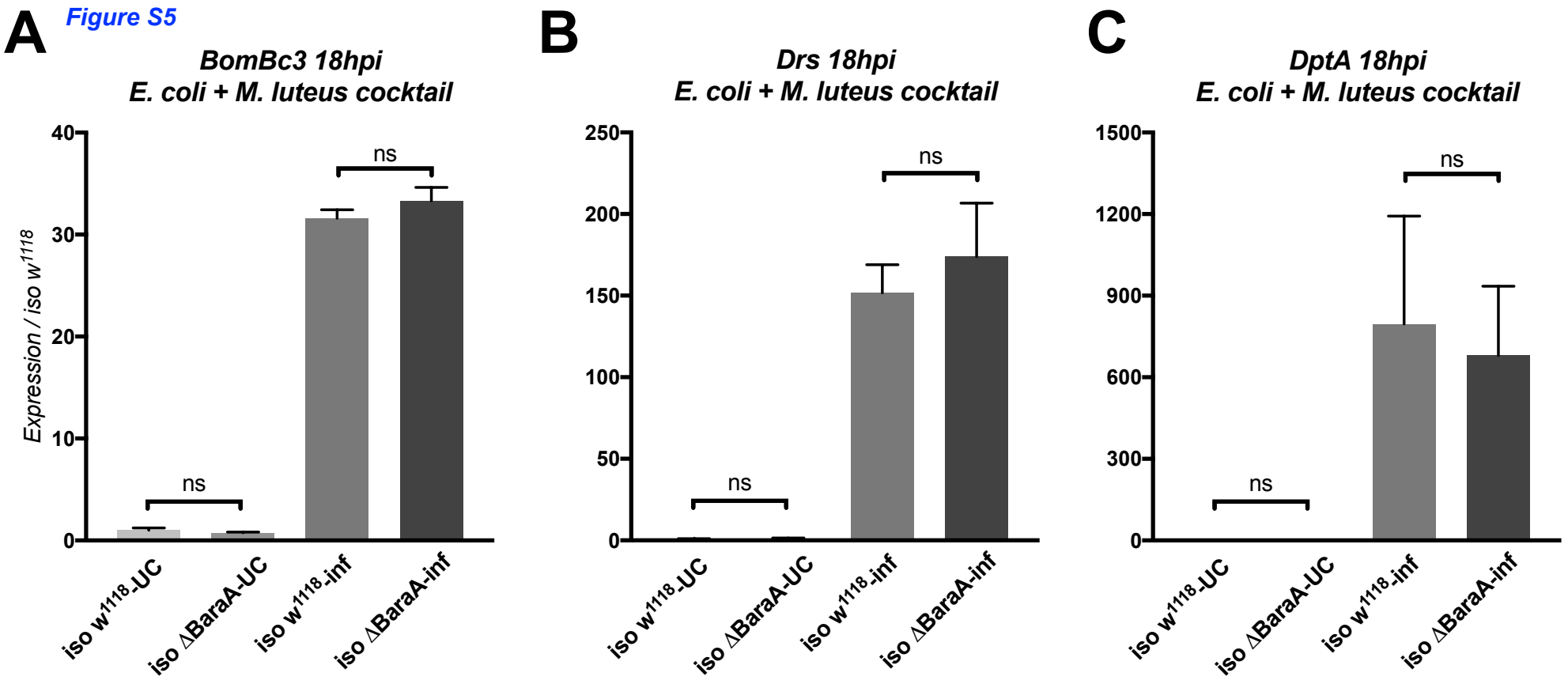
Figure S5
A
BomBc3 18hpi
E. coli + M. luteus cocktail
Expression / iso w1118
40
30
20
10
0
ns
ns
iso w1118-UC
iso ΔBaraA-UC
iso w1118-inf
iso ΔBaraA-inf
B
Drs 18hpi
E. coli + M. luteus cocktail
250
200
150
100
50
0
ns
ns
iso w1118-UC
iso ΔBaraA-UC
iso w1118-inf
iso ΔBaraA-inf
C
DptA 18hpi
E. coli + M. luteus cocktail
1500
1200
900
600
300
0
ns
ns
iso w1118-UC
iso ΔBaraA-UC
iso w1118-inf
iso ΔBaraA-inf

Figure S6

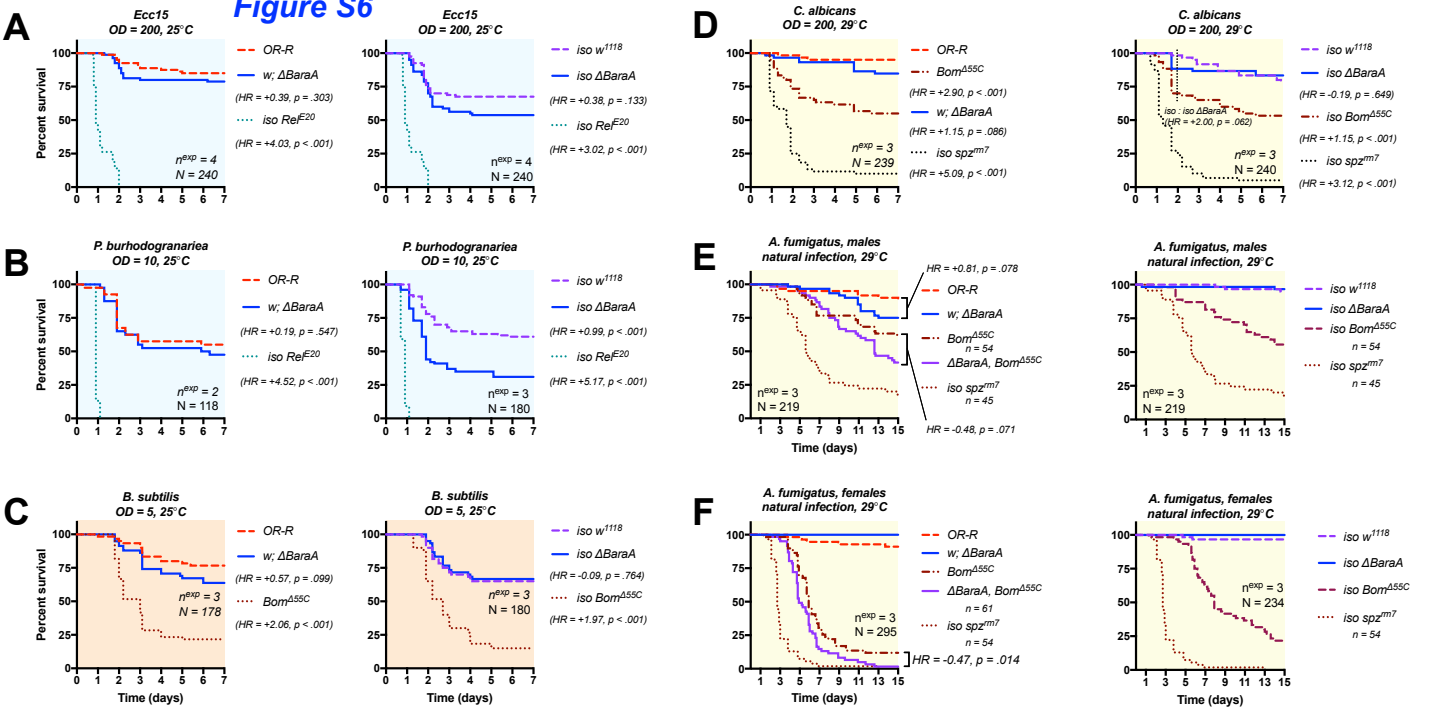
A
Ecc15
OD = 200, 25°C
Percent survival
OR-R
w; ΔBaraA
(HR = +0.39, p = .303)
iso Rel^E20
(HR = +4.03, p < .001)
n^exp = 4
N = 240
Ecc15
OD = 200, 25°C
iso w^1118
iso ΔBaraA
(HR = +0.38, p = .133)
iso Rel^E20
(HR = +3.02, p < .001)
n^exp = 4
N = 240
B
P. burhodogranariea
OD = 10, 25°C
OR-R
w; ΔBaraA
(HR = +0.19, p = .547)
iso Rel^E20
(HR = +4.52, p < .001)
n^exp = 2
N = 118
P. burhodogranariea
OD = 10, 25°C
iso w^1118
iso ΔBaraA
(HR = +0.99, p < .001)
iso Rel^E20
(HR = +5.17, p < .001)
n^exp = 3
N = 180
C
B. subtilis
OD = 5, 25°C
OR-R
w; ΔBaraA
(HR = +0.57, p = .099)
Bom^Δ55C
(HR = +2.06, p < .001)
n^exp = 3
N = 178
Time (days)
B. subtilis
OD = 5, 25°C
iso w^1118
iso ΔBaraA
(HR = -0.09, p = .764)
iso Bom^Δ55C
(HR = +1.97, p < .001)
n^exp = 3
N = 180
Time (days)
D
C. albicans
OD = 200, 29°C
OR-R
Bom^Δ55C
(HR = +2.90, p < .001)
w; ΔBaraA
(HR = +1.15, p = .086)
iso spz^rm7
(HR = +5.09, p < .001)
n^exp = 3
N = 239
C. albicans
OD = 200, 29°C
iso w^1118
iso ΔBaraA
(HR = -0.19, p = .649)
iso : iso ΔBaraA
(HR = +2.00, p = .062)
iso Bom^Δ55C
(HR = +1.15, p < .001)
iso spz^rm7
(HR = +3.12, p < .001)
n^exp = 3
N = 240
E
A. fumigatus, males
natural infection, 29°C
HR = +0.81, p = .078
OR-R
w; ΔBaraA
Bom^Δ55C
n = 54
ΔBaraA, Bom^Δ55C
iso spz^rm7
n = 45
HR = -0.48, p = .071
n^exp = 3
N = 219
Time (days)
A. fumigatus, males
natural infection, 29°C
iso w^1118
iso ΔBaraA
iso Bom^Δ55C
n = 54
iso spz^rm7
n = 45
n^exp = 3
N = 219
F
A. fumigatus, females
natural infection, 29°C
OR-R
w; ΔBaraA
Bom^Δ55C
ΔBaraA, Bom^Δ55C
n = 61
iso spz^rm7
n = 54
HR = -0.47, p = .014
n^exp = 3
N = 295
Time (days)
A. fumigatus, females
natural infection, 29°C
iso w^1118
iso ΔBaraA
iso Bom^Δ55C
iso spz^rm7
n = 54
n^exp = 3
N = 234
Time (days)

Figure S7

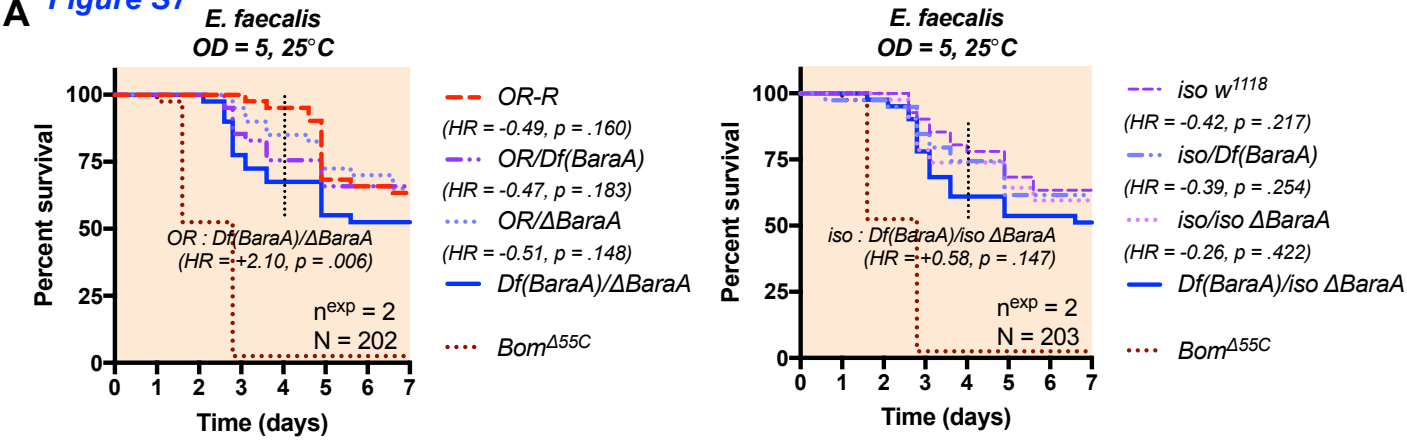
A
E. faecalis
OD = 5, 25°C
Percent survival
Time (days)
OR : Df(BaraA)/ΔBaraA
(HR = +2.10, p = .006)
n^exp = 2
N = 202
OR-R
(HR = -0.49, p = .160)
OR/Df(BaraA)
(HR = -0.47, p = .183)
OR/ΔBaraA
(HR = -0.51, p = .148)
Df(BaraA)/ΔBaraA
Bom^Δ55C
E. faecalis
OD = 5, 25°C
iso : Df(BaraA)/iso ΔBaraA
(HR = +0.58, p = .147)
n^exp = 2
N = 203
iso w^1118
(HR = -0.42, p = .217)
iso/Df(BaraA)
(HR = -0.39, p = .254)
iso/iso ΔBaraA
(HR = -0.26, p = .422)
Df(BaraA)/iso ΔBaraA
Bom^Δ55C

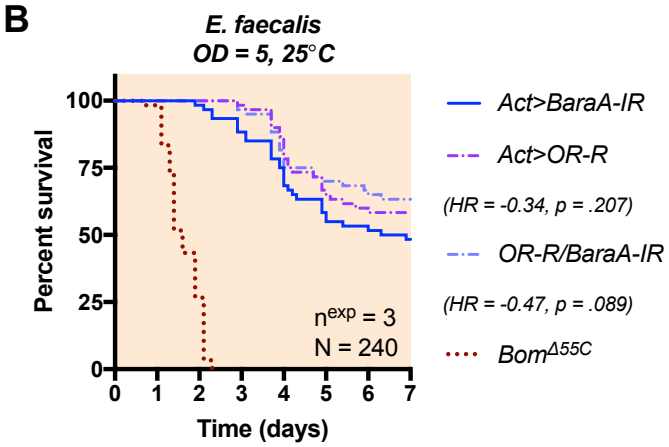
B
E. faecalis
OD = 5, 25°C
Percent survival
Time (days)
n^exp = 3
N = 240
Act>BaraA-IR
Act>OR-R
(HR = -0.34, p = .207)
OR-R/BaraA-IR
(HR = -0.47, p = .089)
Bom^Δ55C

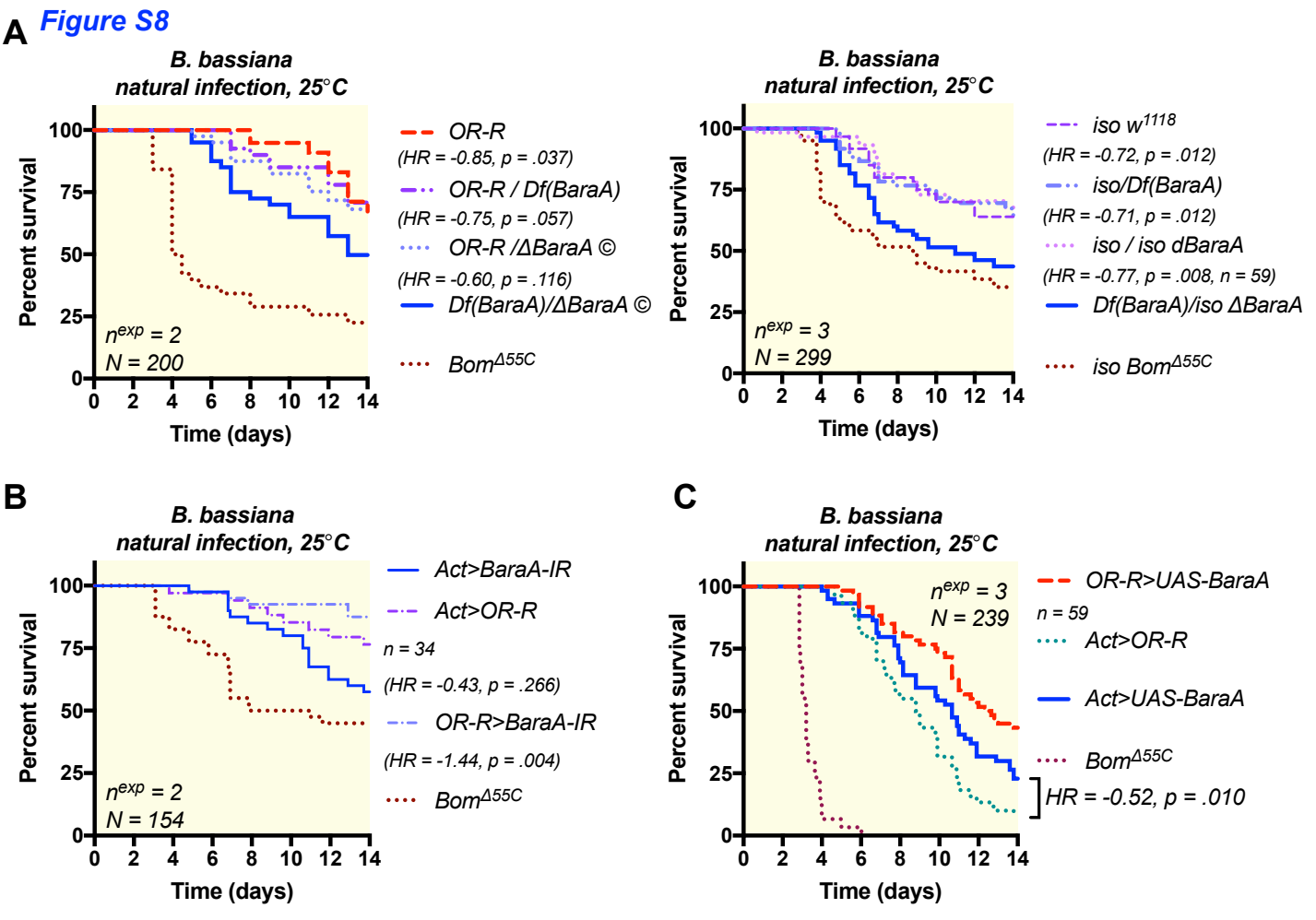
Figure S8
A
B. bassiana
natural infection, 25°C
Percent survival
Time (days)
OR-R
(HR = -0.85, p = .037)
OR-R / Df(BaraA)
(HR = -0.75, p = .057)
OR-R /ΔBaraA ©
(HR = -0.60, p = .116)
Df(BaraA)/ΔBaraA ©
Bom^Δ55C
n^exp = 2
N = 200
B. bassiana
natural infection, 25°C
Percent survival
Time (days)
iso w^1118
(HR = -0.72, p = .012)
iso/Df(BaraA)
(HR = -0.71, p = .012)
iso / iso dBaraA
(HR = -0.77, p = .008, n = 59)
Df(BaraA)/iso ΔBaraA
iso Bom^Δ55C
n^exp = 3
N = 299
B
B. bassiana
natural infection, 25°C
Percent survival
Time (days)
Act>BaraA-IR
Act>OR-R
n = 34
(HR = -0.43, p = .266)
OR-R>BaraA-IR
(HR = -1.44, p = .004)
Bom^Δ55C
n^exp = 2
N = 154
C
B. bassiana
natural infection, 25°C
Percent survival
Time (days)
OR-R>UAS-BaraA
n = 59
Act>OR-R
Act>UAS-BaraA
Bom^Δ55C
HR = -0.52, p = .010
n^exp = 3
N = 239

Figure S9

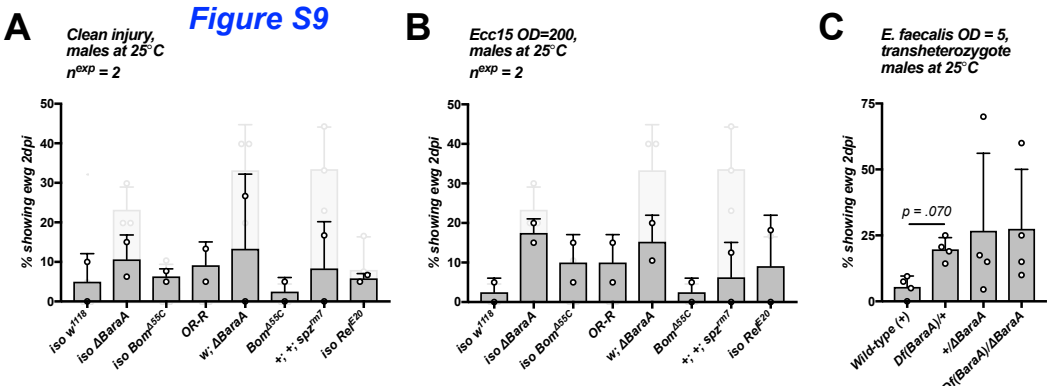
A
Clean injury, males at 25°C
n^exp = 2
% showing ewg 2dpi
50
40
30
20
10
0
iso w^1118
iso ΔBaraA
iso Bom^Δ55C
OR-R
w; ΔBaraA
Bom^Δ55C
+; +; spz^rm7
iso Rel^E20
B
Ecc15 OD=200, males at 25°C
n^exp = 2
% showing ewg 2dpi
50
40
30
20
10
0
iso w^1118
iso ΔBaraA
iso Bom^Δ55C
OR-R
w; ΔBaraA
Bom^Δ55C
+; +; spz^rm7
iso Rel^E20
C
E. faecalis OD = 5, transheterozygote males at 25°C
% showing ewg 2dpi
75
50
25
0
p = .070
Wild-type (+)
Df(BaraA)/+
+/ΔBaraA
Df(BaraA)/ΔBaraA

Table S1

Treatment			***Percent (%) males showing ewg***									
Pathogen	**n exp**	**dpi ewg taken**	***iso DrosDel***	***iso ΔBaraA***	***iso Bom$^{\Delta 55C}$***	***iso spz^{rm7}***	***OR-R***	***w; ΔBaraA***	***Bom$^{\Delta 55C}$***	***+; +; spz^{rm7}***	***iso Rel^{E20}***	***Bom$^{\Delta 55C}$, ΔBaraA***
Clean Injury	2	2	5.0 ± 7.1	10.6 ± 6.2	6.3 ± 1.9		9.2 ± 5.9	13.3 ± 18.9	2.6 ± 3.7	8.3 ± 11.2	5.8 ± 1.2	
HK-E. faecalis (OD100)	3	2	1.7 ± 2.9	23.3 ± 5.8	3.5 ± 6.1		1.7 ± 2.9	33.3 ± 11.6	1.7 ± 2.9	33.6 ± 10.1	8.1 ± 8.3	
E. faecalis (OD5)	4	2	1.3 ± 2.5	23.8 ± 11.1	6.1 ± 1.2		10.5 ± 3.2	60.9 ± 24.4	3.8 ± 4.8	20.2 ± 3.8	3.4 ± 4.1	
B. subtilis	1	2	0.0	30.0	5.0		25.0	40.0	5.0			
A. fumigatus	4 or indicated	6	0.0 ± 0.0	10.6 ± 6.6	2.5 ± 5.0	51.3 ± 15.9 (n=2)	0.0 ± 0.0 (n=3)	50 ± 44.5 (n=3)	0.0 ± 0.0 (n=2)			5.0 ± 7.1 (n=2)
B. bassiana (sporulating plate)	3	3	10.0 ± 0.0	31.5 ± 24.5	11.5 ± 16.0							
B. bassiana R444	3	5	0.0 ± 0.0	15.2 ± 8.7	0.0 ± 0.0		1.7 ± 1.0	15.0 ± 8.6	0.0 ± 0.0	22.2 ± 15.6		14.3 ± 10.0
M. rileyi PHP1705	4 or indicated	5	0.0 ± 0.0 (n=2)	15.0 ± 7.1 (n=2)	2.8 ± 3.9 (n=2)		2.8 ± 3.3	18.1 ± 13.8	0.0 ± 0.0	11.2 ± 8.8		23.2 ± 11.9
Ecc15	2	1	2.5 ± 3.5	17.5 ± 3.5	10.0 ± 7.1		10.0 ± 7.1	15.3 ± 6.7	2.5 ± 3.5	6.3 ± 8.8		

Treatment			***Percent (%) males showing ewg***							
Pathogen	**n exp**	**dpi ewg taken**	***iso DrosDel***	***Df()/iso***	***iso ΔBaraA/iso***	***Df()/iso ΔBaraA***	***OR-R***	***Df()/OR***	***w; ΔBaraA/OR***	***Df()/w; ΔBaraA***
E. faecalis (OD5)	2	2	1.7 ± 2.9	17.4 ± 4.5	11.0 ± 9.2	12.5 ± 3.5	9.0 ± 1.3	22.0 ± 4.2	42.5 ± 38.9	42.5 ± 24.7

Supplementary information:

Identification of the BaraA C-terminus as IM22 from Uttenweiler-Joseph et al.

In 1998, Uttenweiler-Joseph et al. [4] described 24 immune-induced molecules by MALDI-TOF and informed predictions suggested that *BaraA* could encodes several of them [2]. We generated a knock out mutant for the *BaraA* gene (*BaraA*^{SW1}), which we validated by MALDI-TOF peptidomic analysis. Strikingly, we noticed an immune-induced peak at ~5981 Da in Linear mode collections that is absent in *ΔBaraA* flies (**Fig.** 2A); this mass closely resembled the 5984 Da estimated mass of IM22 from Uttenweiler-Joseph et al. [4], for which sequence was never determined. We took the Linear masses reported for then-unknown IMs from Uttenweiler-Joseph et al. [4] and post-hoc generated a standard curve with now-confirmed mass values from Levy et al. [2]. Our post-hoc standard curve corrects the mass of IM22 as found in Uttenweiler-Joseph et al. [4] to be 5973.5 Da. Using the same approach with our own linear data we find a mass of 5975.1 Da for our 5981 Da peak (**Supplementary data file 1**). With LCMS proteomics, we confirmed that the *BaraA* C-terminus is cleaved to remove 4 N-terminal residues, which should produce a putative 5974.5 Da peptide (**Fig** S2). Together these observations indicate the *BaraA* C-terminus encodes the following 53-residue mature peptide, matching the estimated mass of IM22: ARVQGENFVA RDDQAGIWDN NVSVWKRPDG RTVTIDRNGH TIVSGRGRPA QHY.

The *BaraA* gene is therefore involved in the production of over one third of the classical *Drosophila* IMs from Uttenweiler-Joseph et al. [4], including: IM5, 6, 8, 10, 12, 13, 20 (doubly-charged IM24 [2]), 22, and 24.

Sequence of the BaraA-Gal4 promoter construct

The following 1675bp sequence was cloned from the DrosDel isogenic background into the pBPGUw vector to drive a downstream Gal4 gene, and inserted into the VK33 attP docking site using BDSC line #24871:

Dif/dorsal binding site: **GGGHHNNDVH**

Rel binding site: GGRDNNHHBS

>iso_DrosDel_BaraA_promoter-Gal4

CTGCTACTCCTCTACACATTCGACTCCTTCGCCTTGCTGGCTGGGAAAAAATTTTGCATA
ATTTATGTGGGTGCCGCGCACACGGAGGTCCCGACGGATTCGAAGTATCCGAAGGATTCG
AAAGGAAAACAACGCACGAGCACCACGGCCAACTGATTTAAATGCAATTGCACTGAAGT
ATTTTGTTTGGCGAACGAAGCTGGATGAAATAGGGGGGTGTGGGGTTTTCTATTGAGAC
ATCTGCACGTGCAACCGGAAACATCCGAAGAGAACAGCACAGGCCGGGCTACGCCGGGCA
ATTTCTTTTCATTTGCCAAGGTGTTGAGTTGCACCAACATTCGACATCGACGTGGCCAGA
AGCCAACAAAAGCCAAGAGCCAAACCCCTTTTTGTGGTCACAAGTGTCGTCTATTTGTCG
TGGGCATCTTGGGCACCTTGGGCATCCTCGACATCCTTGCCATTTTGGTCTGGCCAAGAC
AAACAACCAGCAAATTTAGTGTATTTTGTGCATTTTTAAAATTGTCCAAATTTATGTGA
CACGCTGCGCCAATTGATCAGATTAAATAAACATGAGGCCAAGCGAATCGAATTTGGCT
TCACCAAGAAGACAATGCAGTCTGTATTCAAATGGGTGGGCGCATCCACCAAGCGGTGA
ATACAGTGACCGCTCGCTATAATGGACGGTCAGGTGTTACTTTAACTTAAAAAAATATG
TAACAAATCTTATCAAGTTTGAAATAGATTGAAATAGATTTGGTTATTGCATTCGAAAG
ATATATATTAAATTCGAATATTCCAAGAAATTTCATGAGAATGTCACTTATGTCATGAG
ATTATATTAACGTACGAATAAACAATGTATTTTCCAAAATTAAAAATAAAATTTAATTT
AATTACGCAGTACCTTTACACTATCAGTCGGAGGTAATAACTCATATAATTAGATTAGC
ATTAGATTTTAAAGCGAAAAACACTTAAAAGCTGAAATTATTAGACAACACTCTTAAAT
TAGTCGAGCTGATATATAGCCTCAAGTTTTGCTTAAATCCAAAGATAAAGGAATGCCTT
CAAAAATATATTTTGTTTTATACCAAGTGACAGCAGAGAATGGGGTTGCAATATCTTAA
AAGAGTTTCACTTAGCCAATATTTACTGCCATTGTTGGCCACCAAATAGTAGCAACCAGA
GACTTCCAGGAATATATTCTCGTGTCAAATGCAATCCACTTTAAATGCAACTATCTGGCG
GCTAAGAAAACCCGACAGTTTGATTCAAGTCGACGAAACAATATAAGCACGTGCTAAAT
AAAGAGACCTATGCAGTTAATACTCTTGTCATATTATAATATAATTTAGTGACATAAGT
TGCATGGTATACGAGTACTGAACAAGTTATGGCAGCTTTTCCAAATAAGCGATCACATA
TTCCGCGGGATGATGGGTGGATTTCTAGCATATGTGGATGCTTAATGGCTTATTGC**GGG**
TCAGGGCGGCGCAATCTGTTC**AGAAATTCCC**GAACGCACACCCATTTCAGATCAGATTG
TGACGTTTT**GGGAAATTCT**TGACGATCGGTGTAAACAAGCTCAGCAACCAGATTCGATG
GCTATTTGCCGGCTATAAATACTAGAAACCATTCGATTGCACTCAGTTGAAGCTGGGCTC
TGGAACAGATCACA